SUPLEMENTARY INFORMATION

Synthesis of Locked Cyclohexene and Cyclohexane Nucleic Acids (LCeNA and LCNA)

Michal Šála*, Milan Dejmek, Eliška Procházková, Hubert Hřebabecký, Jiří Rybáček, Martin Dračínský, Pavel Novák, Šárka Rosenbergová, Jiří Fukal, Vladimír Sychrovský, Ivan Rosenberg, Radim Nencka*

Institute of Organic Chemistry and Biochemistry, Academy of Sciences of the Czech Republic, v.v.i., Gilead Sciences & IOCB Research Centre, Czech Republic.

sala@uochb.cas.cz, *nencka@uochb.cas.cz*

Contents

Determination of the optical purity of the compound 8b

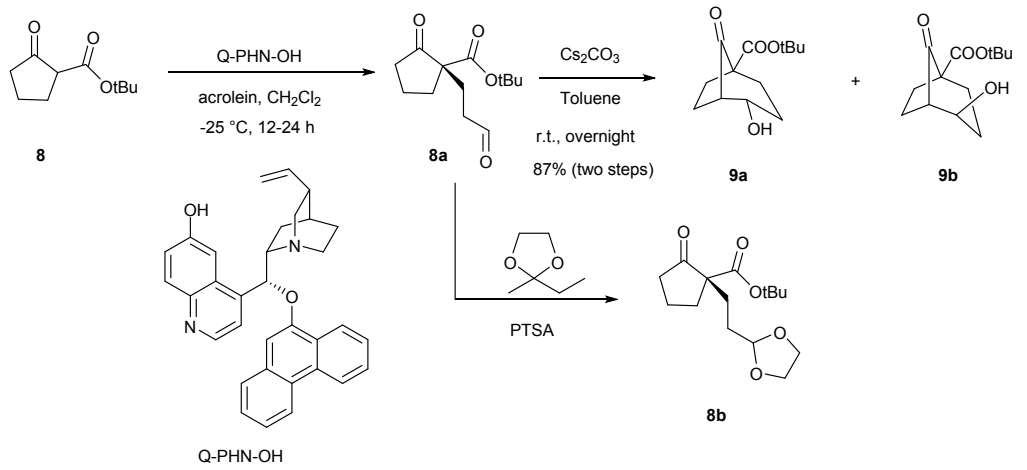

To a mixture of starting material **8** (9.05 g, 49.1 mmol) and catalyst Q-PHN-OH[1] (2.40 g, 4.93 mmol, 0.1 eq.) in dry CH_2Cl_2 (100 mL) at - 25 °C under argon atmosphere, a solution of acrolein (8.23 mL, 123 mmol, 2.5 eq.) in CH_2Cl_2 (30 mL) was added dropwise. Reaction mixture was occasionally stirred (>95% of time without stirring) and kept at -25 °C for 24 h. Then the reaction mixture was poured onto silica gel column (200 g, Et_2O) and crude product was eluted with Et_2O. Fractions containing product were collected and evaporated to afford crude **8a** (12.53 g) which was used immediately in the next step. Crude catalyst was then eluted from the column with methanol and recycled (chromatography on silica gel column in CH_2Cl_2:ethanol 25:1).

Crude product **8a** was dissolved in toluene (350 mL), cesium carbonate (8.48 g, 26 mmol) was added and the reaction mixture was stirred at r.t. overnight. Solids were removed by filtration through Celite and the filtrate was evaporated. Product was purified on a siliga gel column (250 g, toluene:ethylacetate 3:1 → 2:1) to afford 9.416 g (80%) of the mixture **9a** and **9b** (Figure **S1**.) Analytical samples of both isomers were obtained by column chromatography of the sample (300 mg of the mixture, 100 g of silica gel, toluene:ethylacetate 3:1 → 2:1).

Determination of optical purity – preparation of compound **8b**.

Crude aldehyde intermediate **8a** (250 mg) in 2-ethyl-2-methyl-1,3-dioxolane (0.3 mL) was stirred at r.t. with *p*-TsOH (9 mg) for 45 min. Then the reaction mixture was diluted with diethyl ether (30 mL) and washed with saturated sodium bicarbonate solution (10 mL). Organic phase was dried with sodium sulfate and evaporated. Residue was purified by chromatography (50 g) in pentane:ether (2:1) and the obtained product **8b** was analyzed by

chiral HPLC (Eurocel 01 Knauer, in hexane: *i*-PrOH 97:3, Fig. **S2**, **S3**). NMR spectra match those reported[1].

Synthesis and hybridization properties of the homooligomers ($\underline{A_9}$)

Synthesis of homooligomers

Adenine homooligomers were synthesized using UNYLINKER solid support (Glen Res.). Gaseous ammonia (0.7 MPa) cleavage of the oligoadenylate from this support proceeded well, however, MALDI TOF (Table **S2**, Figure **S1**) revealed residual part of the linker attached to the 3'-end of oligoadenylate analog. Oligonucleotides were purified at 55°C on DNAPac PA100 10 x 250 mm Nucleic Acid Column (Dionex) at a flow rate of 3 mL/min using a linear gradient od sodium chloride (20 mM→500 mM, 60 min) in 50 mM sodium acetate buffer pH 7.0 containing 20% (v) of acetonitrile. Desalting of pure oligonucleotides was performed on 10 μm Luna C18 (2) 10 x 100 mm column (Phenomenex) at a flow rate of 3 mL/min using a gradient of acetonitrile (0→25%, 30 min) in 0.1 M triethylammonium hydrogencarbonate. Desalted oligonucleotides were freeze-dried and characterized by MALDI TOF (Table **S1**.).

Table **S1**. Analytical data for oligonucleotides

Oligonucleotide	Calcd. mass	Found mass
$(\underline{\mathbf{A}^{25}})_9$[a]	3342.70	3343.8
$(\underline{\mathbf{A}^{25}})_9$[a]	3360.83	3360.0

[a] Oligomer contained residual part of the linker, see Figure **S1**.

Hybridization properties of homooligomers ($\underline{A_9}$)

The denaturation experiments showed again strongly destabilization effect (Table **S2.**). We also measured behaviour of the modified homooligomer $(\mathbf{A}^{25})_9$ in solution without complementary chain (T_9). From observation of the hyperchromic effects (modified homooligomer $(\mathbf{A}^{25})_9$ ~ 0.04, natural A_9 ~ 0.12) we assume that the T_m of the modified homooligomer is independent on the presence of the complementary chain in the mixture and there is no duplex formation.

Table S2. Thermal stability of modified oligonucleotide duplexes[a]

Oligonucleotide[c]	ssRNA T_m (ΔT_m)[b]	ssDNA T_m (ΔT_m)[b]
(**A**^{25})$_9$	no comp. form.	no comp. form.
(**A**^{26})$_9$	no comp. form.	no comp. form.

[a] 4 μM duplex in 50 mM NaH_2PO_4 – Na_2HPO_4 pH 7.2 with 100 mM NaCl; [b] per modification; [c] Oligomer contained residual part of the linker, see Figure **S1**.

Figure **S1**. Structures of the homooligomers with attached residual part from the linker

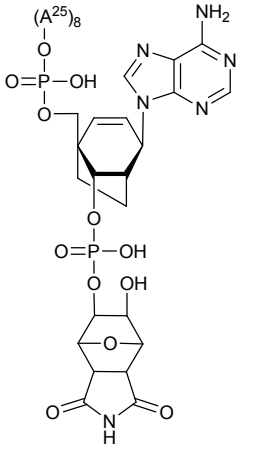

(**A**^{25})$_9$

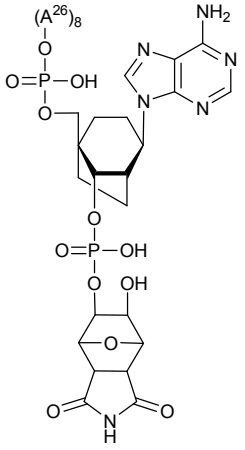

(**A**^{26})$_9$

Molecular dynamic calculations (experimental part)

The structural models of normal RNA-RNA oligonucleotide, oligonucleotide containing A5 adenosine residue with modified sugar and oligonucleotide containing A3, A5, and A8 modified residues were prepared employing the structure with PDB ID 1HG9 for RNA-DNA molecule that have similar sequence end length as the studied molecules. The three structural models were prepared by structure editing of original 1HG9 structure employing the Avogadro software. The parameterization of force-field for the chemically modified sugar moieties was based on ESP population analysis employing the Hartree-Fock method and the 6-31g(d,p) basis. The standard parmbsc0 force field was employed for all other residues. The three constructs were solvated by TIP3P water in a 15 Å x 15 Å x 15 Å box and negative charges of phosphate groups were compensated by added Na+ ions by employing xLEaP software.

Each of the systems was firstly equilibrated employing following protocol. The RNA construct was restrained (force constant 25 kcal/mol) and heated from 100 K to 300 K during 100 ps molecular dynamic run. Then, minimization followed by short equilibration lasting 50 ps was performed five times with decreasing force constant up to 1 kcal/mol. Then, 100 ps dynamics employing force constant 0.5 kcal/mol was performed. The equilibration process lasting in total 500 ps was finished by unconstrained 50 ps dynamics. After the equilibration the 20 ns production dynamics for all three constructs has been calculated. All the molecular dynamic calculations using Amber 10 program ware carried out at standard laboratory conditions; temperature 298.15 K, pressure 1 atm.

Figure **S2**. GC chromatogram of the mixture of **9a** and **9b**.

```
File       :D:\Data\MS_cyclization_21_07.D
Operator   : Galeta
Acquired   : 21 Jul 2014  13:54     using AcqMethod AS_M-NIZKE_C-VYSOKE.M
Instrument :    6890N + 5975B
Sample Name: MS_cyclization_21_07
Misc Info  :
Vial Number: 5
```

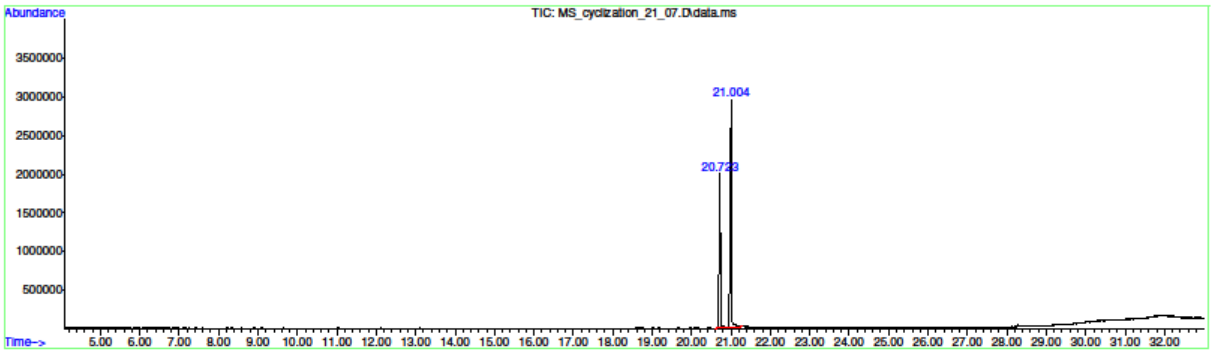

Area Percent Report

```
Data Path : D:\Data\
Data File : MS_cyclization_21_07.D
Acq On    : 21 Jul 2014  13:54
Operator  : Galeta
Sample    : MS_cyclization_21_07
Misc      :
ALS Vial  : 5   Sample Multiplier: 1

Integration Parameters: autoint1.e
Integrator: ChemStation

Method    : D:\Data\PP-P617-3.D\AS_M-VYSOKE_C-VYSOKE.M
Title     :

Signal     : EIC TIC: MS_cyclization_21_07.D\data.ms
```

peak #	R.T. min	first scan	max scan	last scan	PK TY	peak height	corr. area	corr. % max.	% of total
1	20.723	1300	1309	1320	BV	1960426	43452777	63.77%	38.939%
2	21.004	1320	1331	1353	VV	2641477	68138671	100.00%	61.061%

```
                          Sum of corrected areas:    111591448

AS_M-VYSOKE_C-VYSOKE.M Tue Jul 22 11:54:34 2014 CHEMSTATION
```

Figure **S3**. Chromatogram of racemic mixture of **8b**.

11.7.2013 15:00 Chromatogram C:\Clarity\Work1\DATA\MS-RAC-03-07_EC1_01.PRM Page 1 of 1

Sample Info:

Sample ID	: MS-RAC-03-07	Amount	: 0
Sample	: MS-racemat	ISTD Amount	: 0
Inj. Volume [ml]	: 0	Dilution	: 1
Column	: Eurocel 01 (Knauer) 250 x 4.6 mm, 5 um	Detection	: Chiralyser + UV 220 nm
Mobile Phase	: hexane : i-PrOH = 97 : 3	Temperature	:
Flow Rate	: 1.0 mL/min	Pressure	: 30 atm
Note	:		

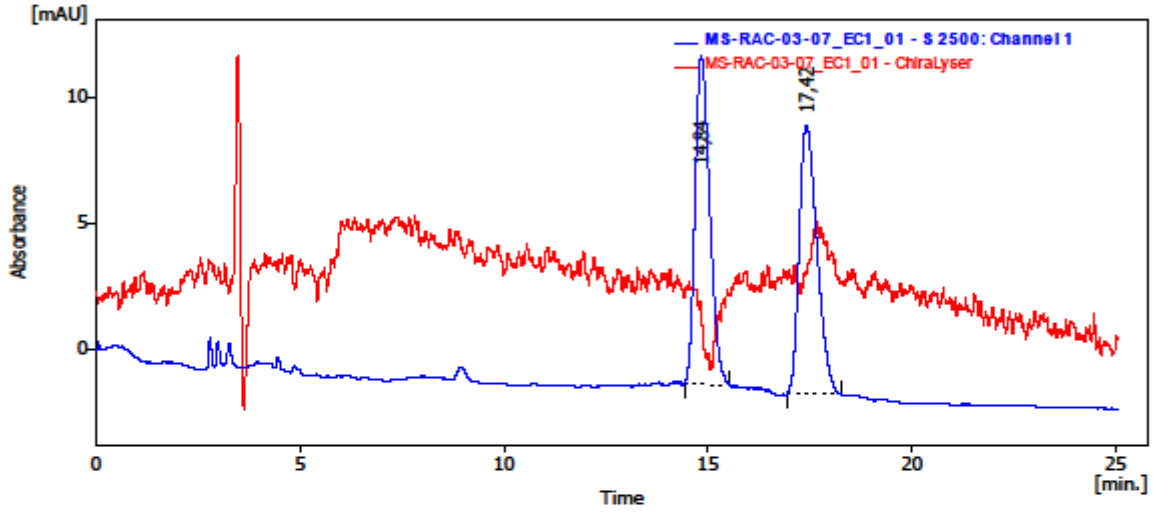

Result Table (Uncal - MS-RAC-03-07_EC1_01 - S 2500: Channel 1)

	Reten. Time [min]	Area [mAU.s]	Height [mAU]	Area [%]	Height [%]	W05 [min]
1	14,840	323,75	13,078	50,0	55,0	0,40
2	17,420	323,46	10,688	50,0	45,0	0,48
	Total	647,20	23,767	100,0	100,0	

Figure **S4**. Chromatogram of **8b**.

11.7.2013 15:28 Chromatogram C:\Clarity\Work1\DATA\MS-S-03-07_EC1_01.PRM Page 1 of 1

Sample Info:

Sample ID	: MS-RAC-03-07	Amount	: 0
Sample	: MS-racemat	ISTD Amount	: 0
Inj. Volume [ml]	: 0	Dilution	: 1
Column	: Eurocel 01 (Knauer) 250 x 4.6 mm, 5 um	Detection	: Chiralyser + UV 220 nm
Mobile Phase	: hexane : i-PrOH = 97 : 3	Temperature	:
Flow Rate	: 1.0 mL/min	Pressure	: 30 atm
Note	:		

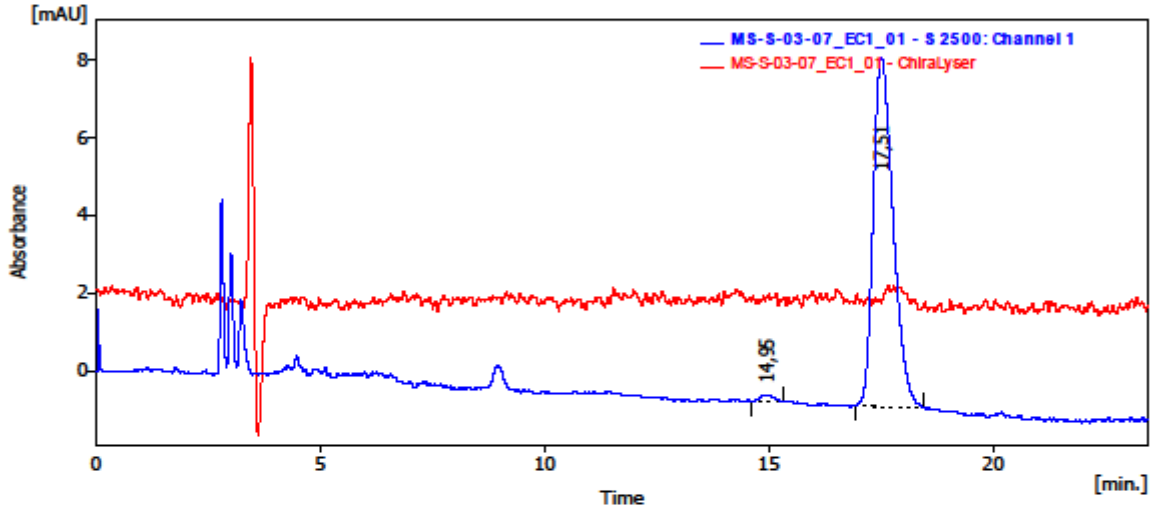

Result Table (Uncal - MS-S-03-07_EC1_01 - S 2500: Channel 1)

	Reten. Time [min]	Area [mAU.s]	Height [mAU]	Area [%]	Height [%]	W05 [min]
1	14,953	3,56	0,169	1,3	1,8	0,37
2	17,513	277,11	8,985	98,7	98,2	0,48
	Total	280,66	9,154	100,0	100,0	

Figure **S5**. Separation of racemic nucleoside **25** on chiral HPLC column. Sample of the racemic nucleoside **25** was prepared using completely the same synthetic scheme and procedures only the conversion of **8** to mixture of **9a**/**9b** was done in an achiral way according to the published protocol[2].

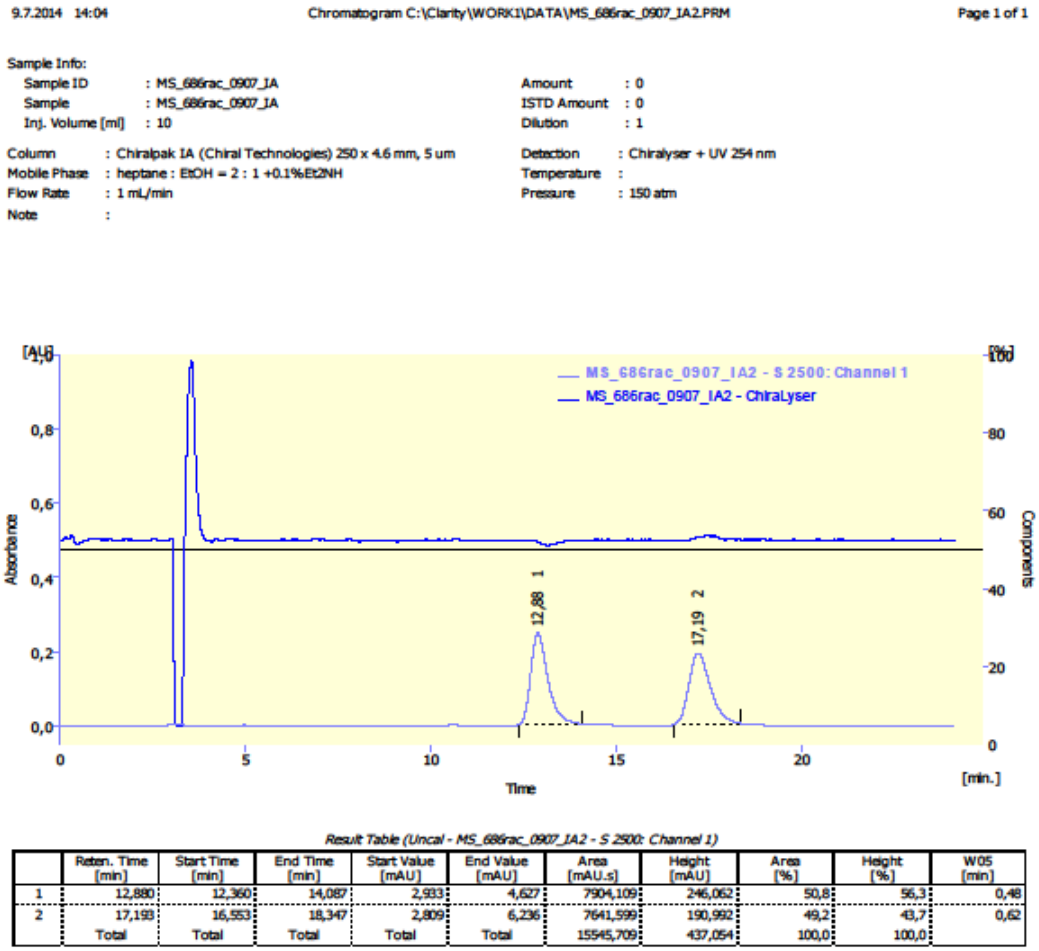

Result Table (Uncal - MS_686rac_0907_IA2 - S 2500: Channel 1)

	Reten. Time [min]	Start Time [min]	End Time [min]	Start Value [mAU]	End Value [mAU]	Area [mAU.s]	Height [mAU]	Area [%]	Height [%]	W05 [min]
1	12,880	12,360	14,087	2,933	4,627	7904,109	246,062	50,8	56,3	0,48
2	17,193	16,553	18,347	2,809	6,236	7641,599	190,992	49,2	43,7	0,62
	Total	Total	Total	Total	Total	15545,709	437,054	100,0	100,0	

Figure **S6**. Separation of nucleoside **25** (single enantiomer) on chiral HPLC column

9.7.2014 14:04 Chromatogram C:\Clarity\WORK1\DATA\MS_686enant_0907_IA.PRM Page 1 of 1

Sample Info:

Sample ID	: MS_686rac_0907_IA_en	Amount	: 0
Sample	: MS_686rac_0907_IA_en	ISTD Amount	: 0
Inj. Volume [ml]	: 10	Dilution	: 1
Column	: Chiralpak IA (Chiral Technologies) 250 x 4.6 mm, 5 um	Detection	: Chiralyser + UV 254 nm
Mobile Phase	: heptane : EtOH = 2 : 1 +0.1%Et2NH	Temperature	:
Flow Rate	: 1 mL/min	Pressure	: 150 atm
Note	:		

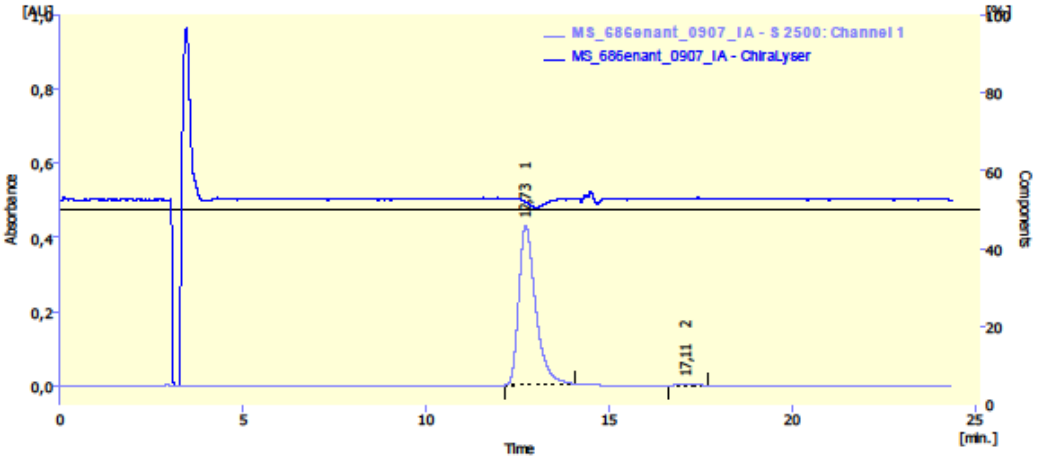

Result Table (Uncal - MS_686enant_0907_IA - S 2500: Channel 1)

	Reten. Time [min]	Start Time [min]	End Time [min]	Start Value [mAU]	End Value [mAU]	Area [mAU.s]	Height [mAU]	Area [%]	Height [%]	W05 [min]
1	12,727	12,153	14,087	0,696	4,577	13796,128	430,442	99,2	99,3	0,48
2	17,113	16,640	17,700	0,595	0,714	107,352	3,156	0,8	0,7	0,57
	Total	Total	Total	Total	Total	13903,481	433,599	100,0	100,0	

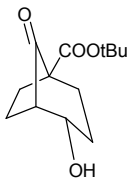
O
COOtBu
OH

9a

5.5
5.0
4.5
4.0
3.5
3.0
2.5
2.0
1.5
1.0
0.5
ppm
1.0
1.0
1.2
0.8
1.1
5.2
1.1
9.4

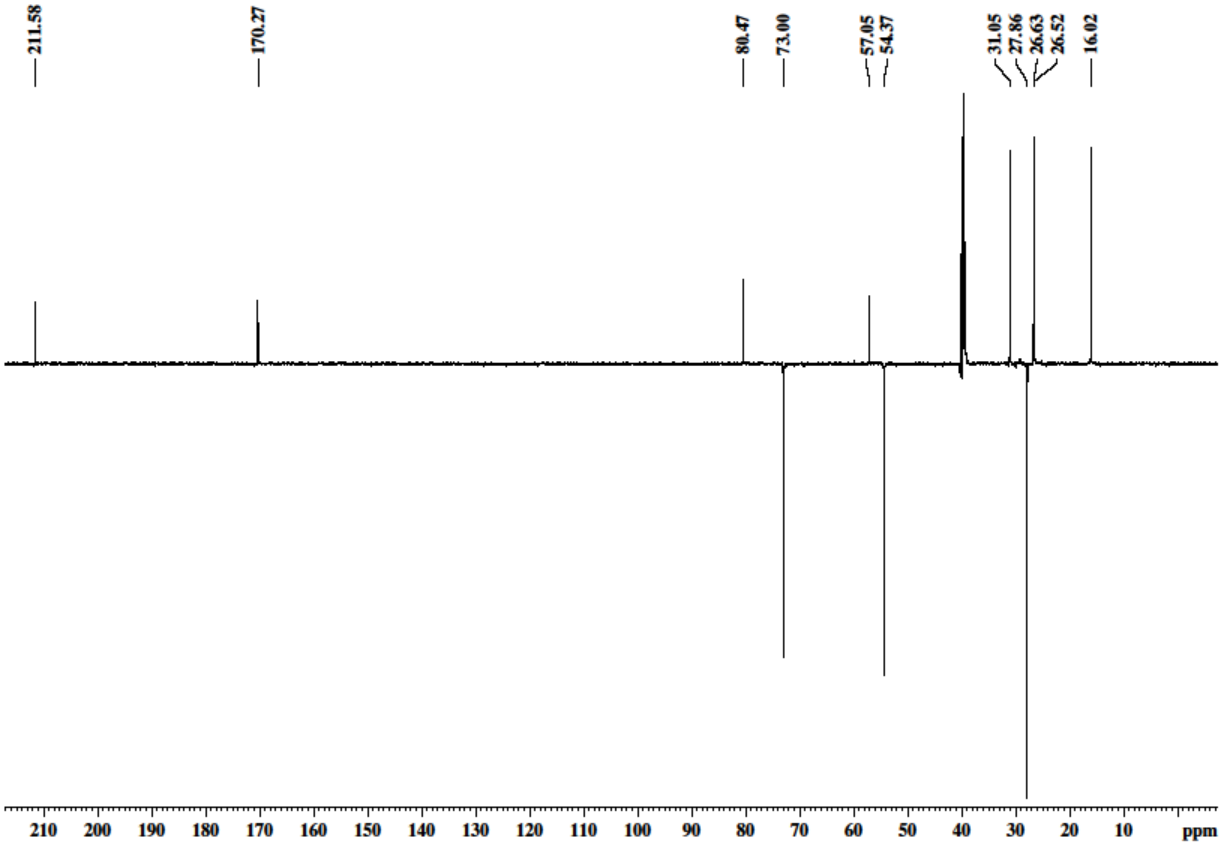
211.58
170.27
80.47
73.00
57.05
54.37
31.05
27.86
26.63
26.52
16.02
210
200
190
180
170
160
150
140
130
120
110
100
90
80
70
60
50
40
30
20
10
ppm

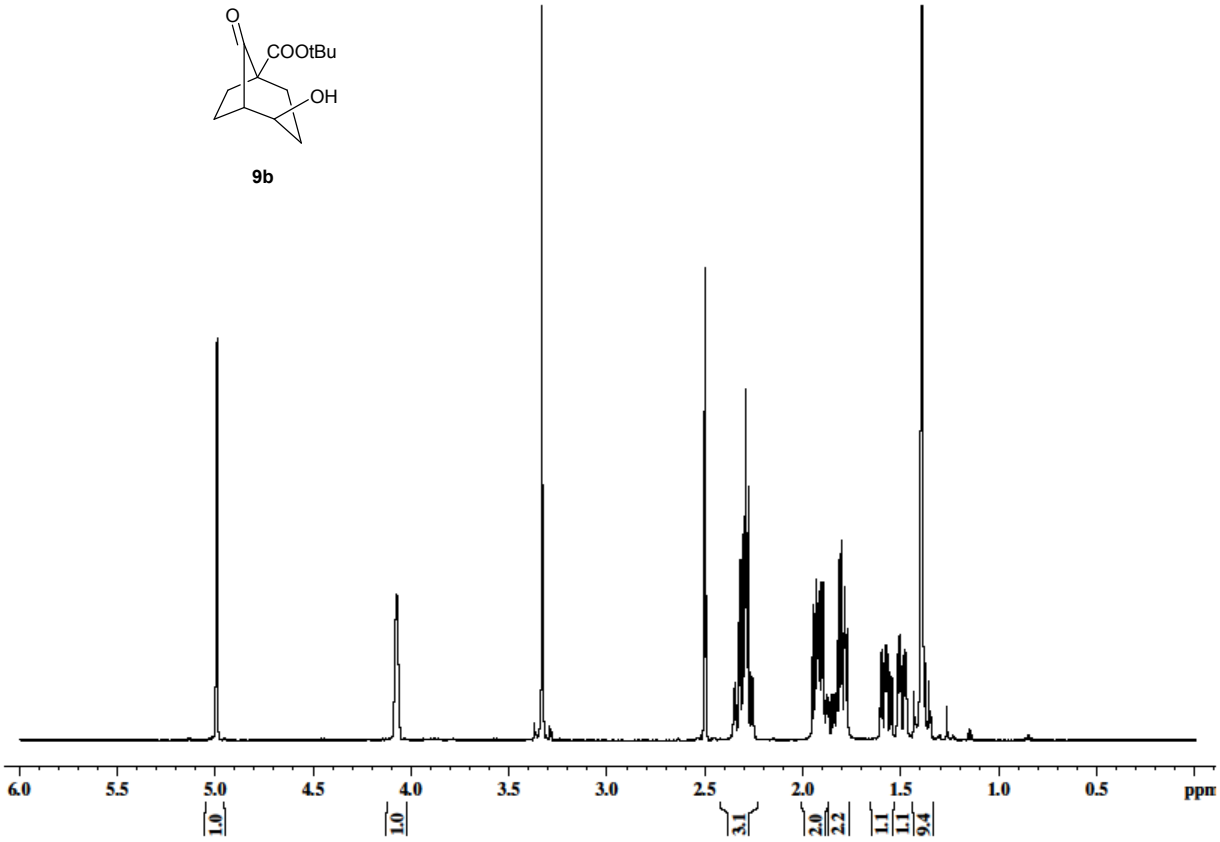
O
COOtBu
OH
9b
6.0
5.5
5.0
4.5
4.0
3.5
3.0
2.5
2.0
1.5
1.0
0.5
ppm
1.0
1.0
3.1
2.0
2.2
1.1
1.1
9.4

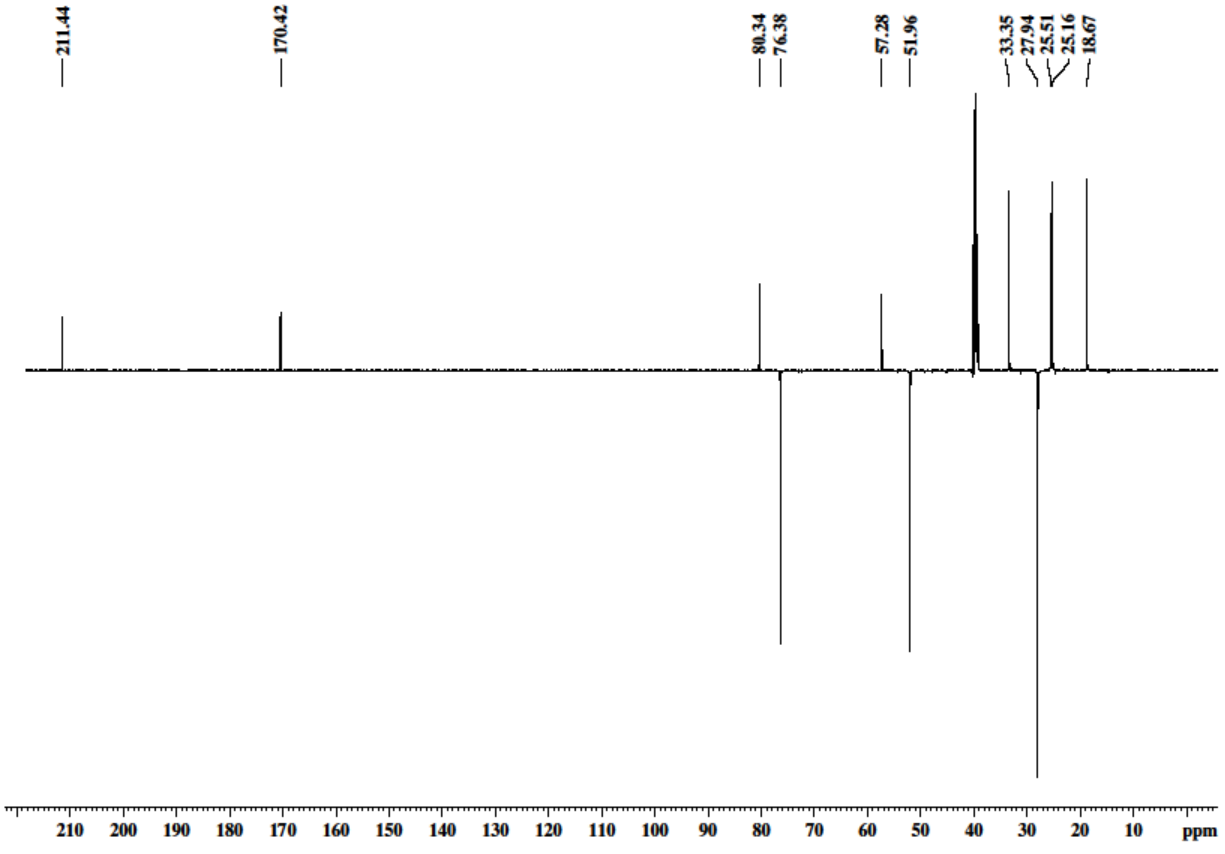
211.44
170.42
80.34
76.38
57.28
51.96
33.35
27.94
25.51
25.16
18.67
210
200
190
180
170
160
150
140
130
120
110
100
90
80
70
60
50
40
30
20
10
ppm

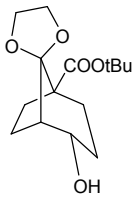
O
O
COOtBu
OH

10a

5.5
5.0
4.5
4.0
3.5
3.0
2.5
2.0
1.5
1.0
0.5
ppm
1.0
4.1
1.0
1.0
1.0
1.0
1.0
1.0
2.3
9.3
0.7
1.1

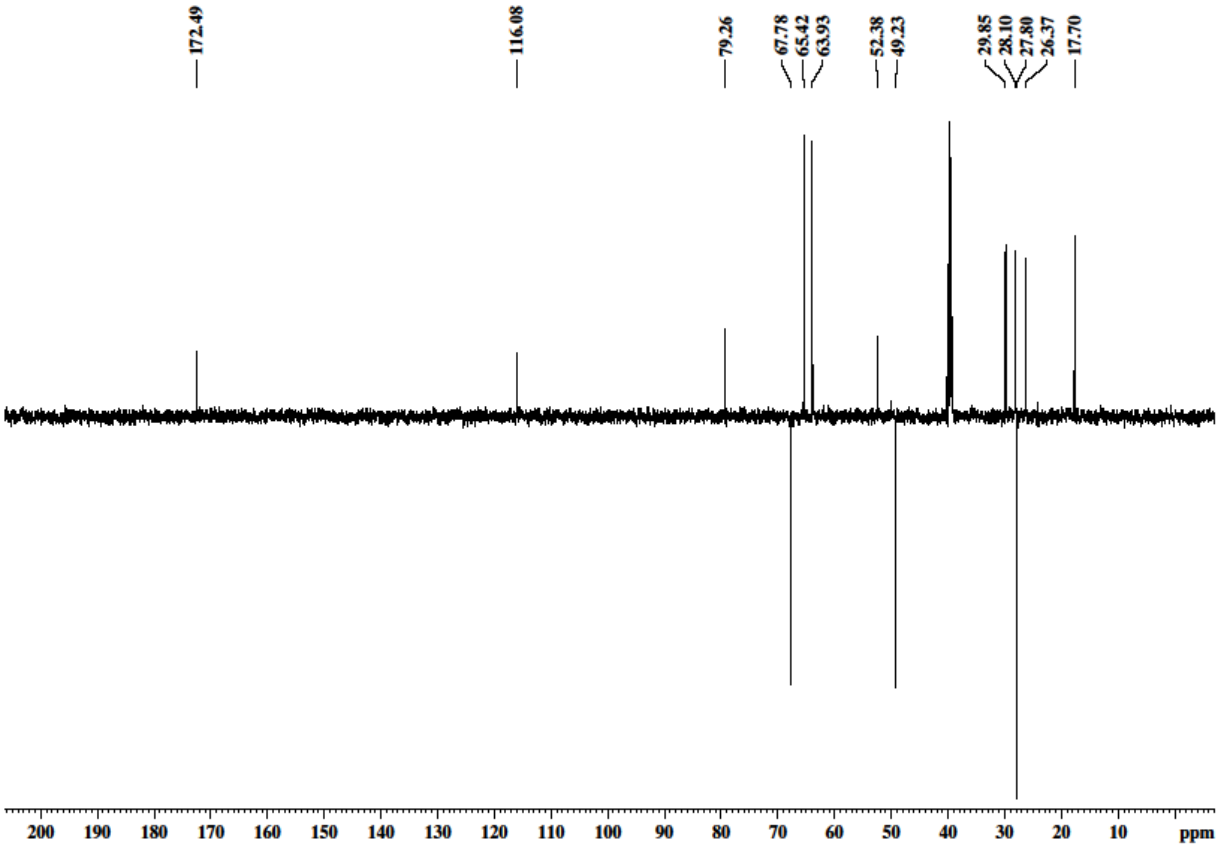
172.49
116.08
79.26
67.78
65.42
63.93
52.38
49.23
29.85
28.10
27.80
26.37
17.70
200
190
180
170
160
150
140
130
120
110
100
90
80
70
60
50
40
30
20
10
ppm

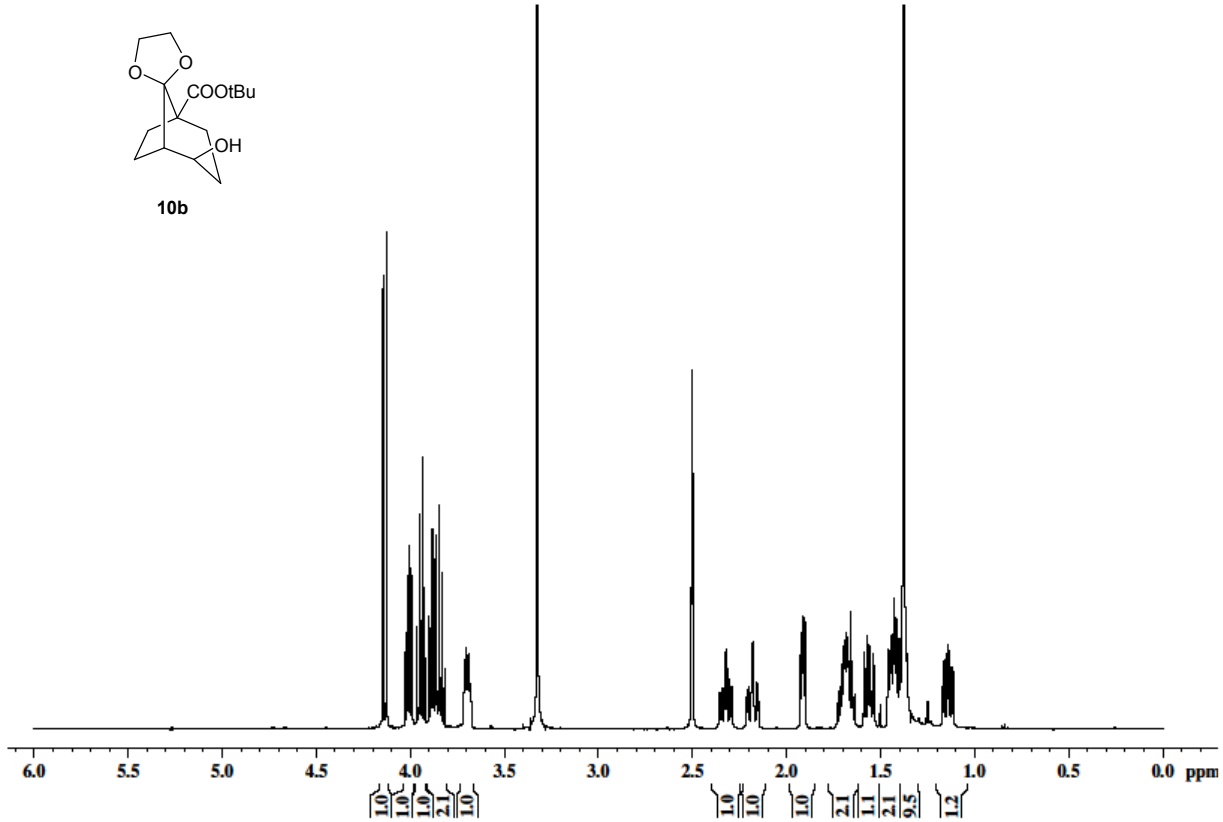
O
O
COOtBu
OH
10b
6.0
5.5
5.0
4.5
4.0
3.5
3.0
2.5
2.0
1.5
1.0
0.5
0.0 ppm
1.0
1.0
1.0
2.1
1.0
1.0
1.0
1.0
2.1
1.1
2.1
9.5
1.2

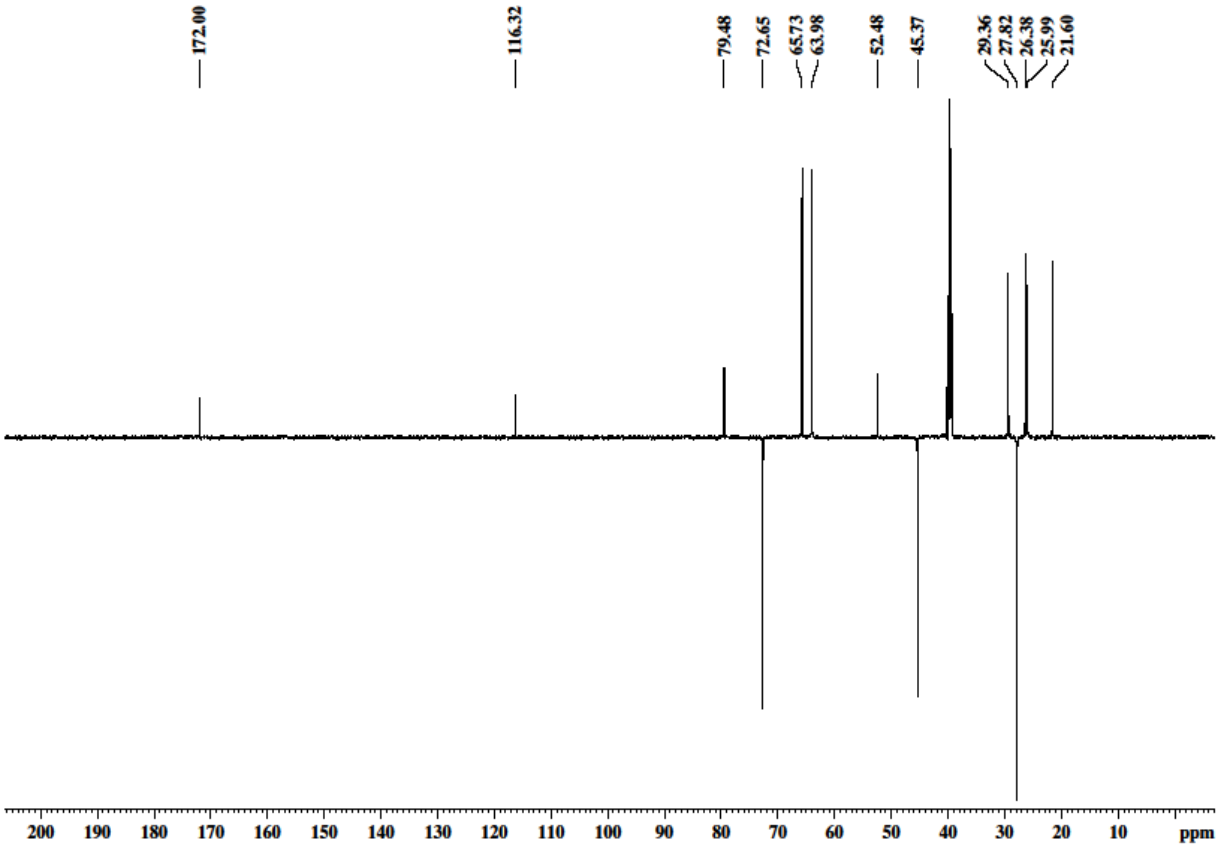
172.00
116.32
79.48
72.65
65.73
63.98
52.48
45.37
29.36
27.82
26.38
25.99
21.60
200
190
180
170
160
150
140
130
120
110
100
90
80
70
60
50
40
30
20
10
ppm

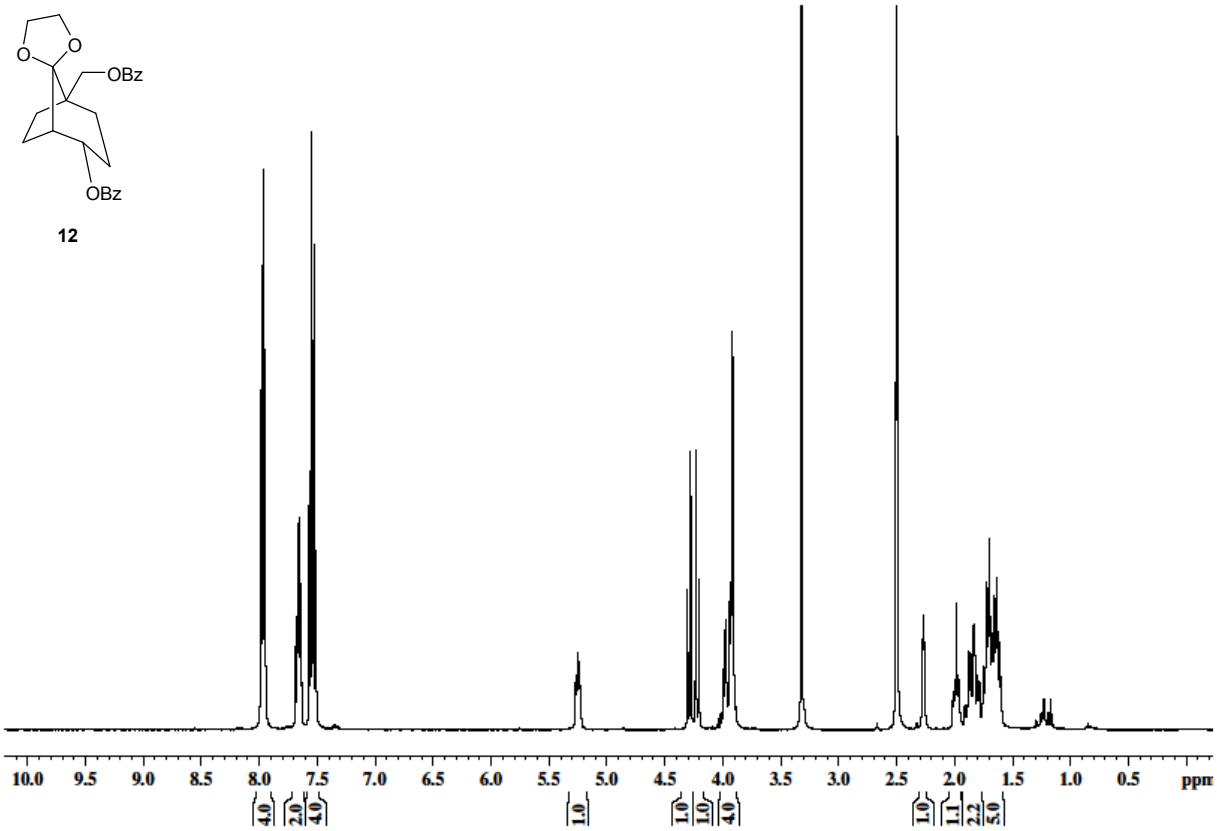
OBz
OBz
12
10.0 9.5 9.0 8.5 8.0 7.5 7.0 6.5 6.0 5.5 5.0 4.5 4.0 3.5 3.0 2.5 2.0 1.5 1.0 0.5 ppm
4.0 2.0 4.0 1.0 1.0 1.0 4.0 1.0 1.1 2.2 5.0

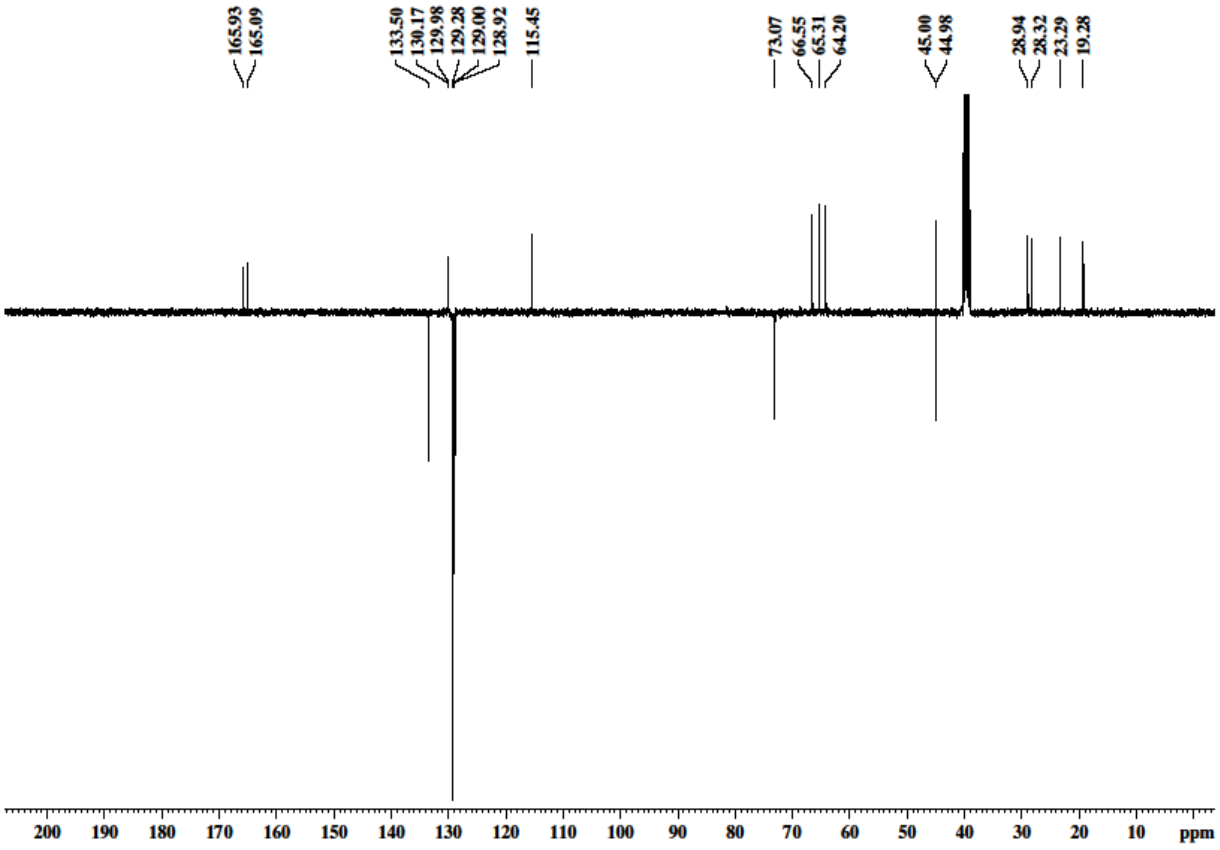
165.93
165.09
133.50
130.17
129.98
129.28
129.00
128.92
115.45
73.07
66.55
65.31
64.20
45.00
44.98
28.94
28.32
23.29
19.28
200 190 180 170 160 150 140 130 120 110 100 90 80 70 60 50 40 30 20 10 ppm

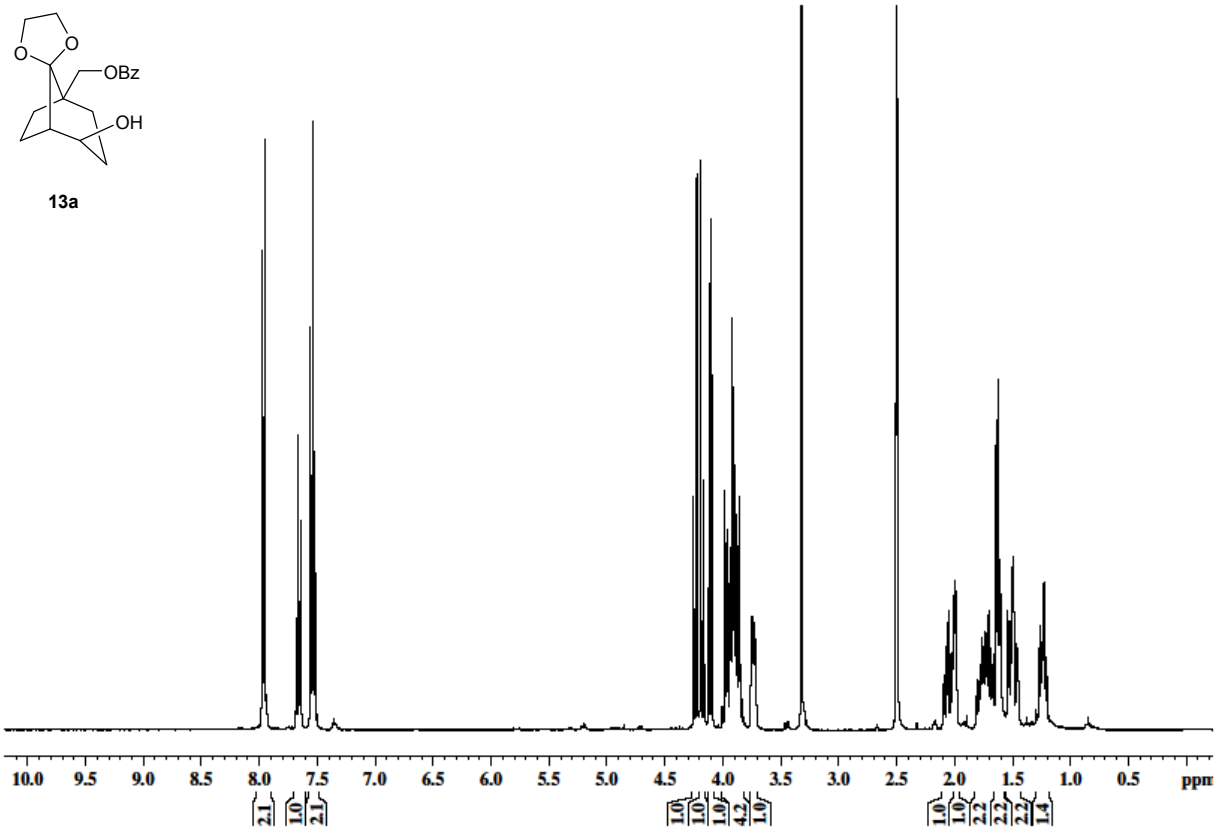
OBz
OH
10.0 9.5 9.0 8.5 8.0 7.5 7.0 6.5 6.0 5.5 5.0 4.5 4.0 3.5 3.0 2.5 2.0 1.5 1.0 0.5 ppm
2.1 1.0 2.1 1.0 1.0 1.0 4.2 1.0 1.0 1.0 2.2 2.2 2.2 1.4

13a

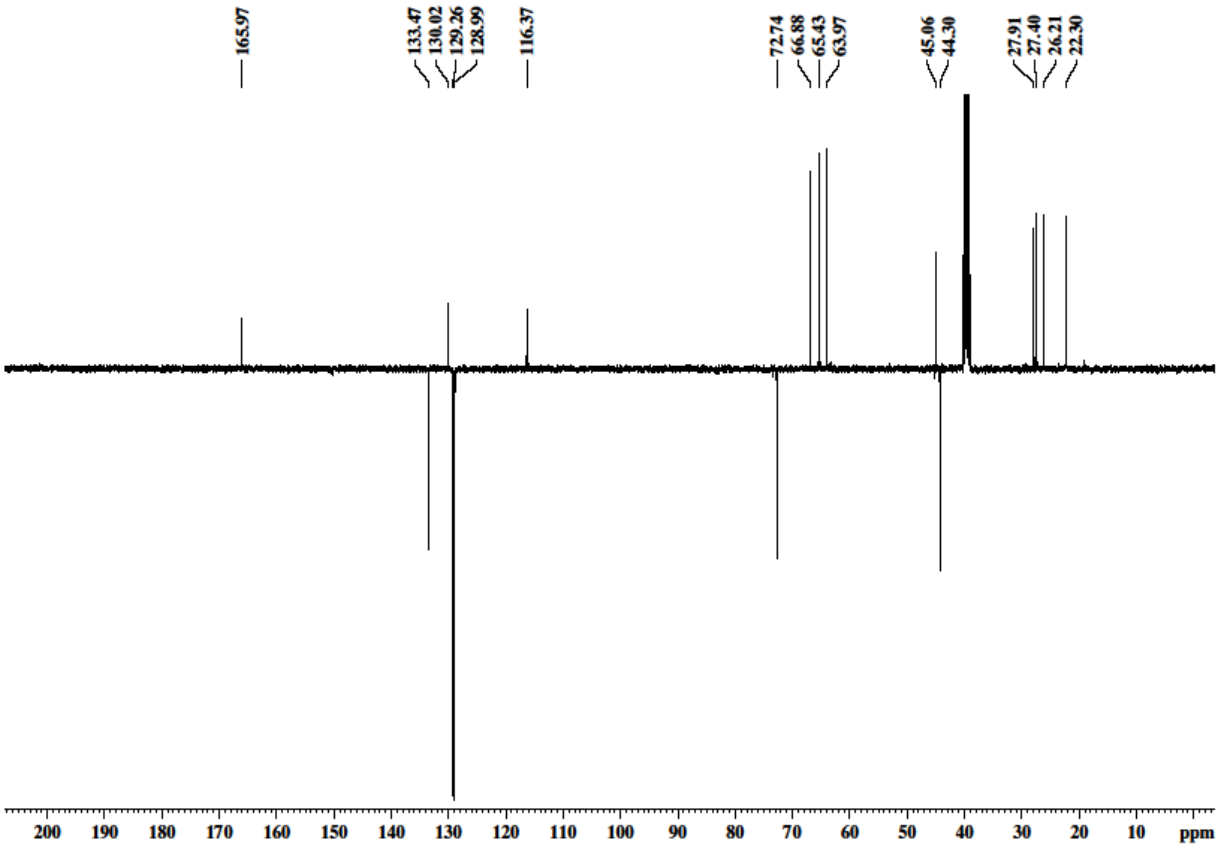
165.97
133.47
130.02
129.26
128.99
116.37
72.74
66.88
65.43
63.97
45.06
44.30
27.91
27.40
26.21
22.30
200 190 180 170 160 150 140 130 120 110 100 90 80 70 60 50 40 30 20 10 ppm

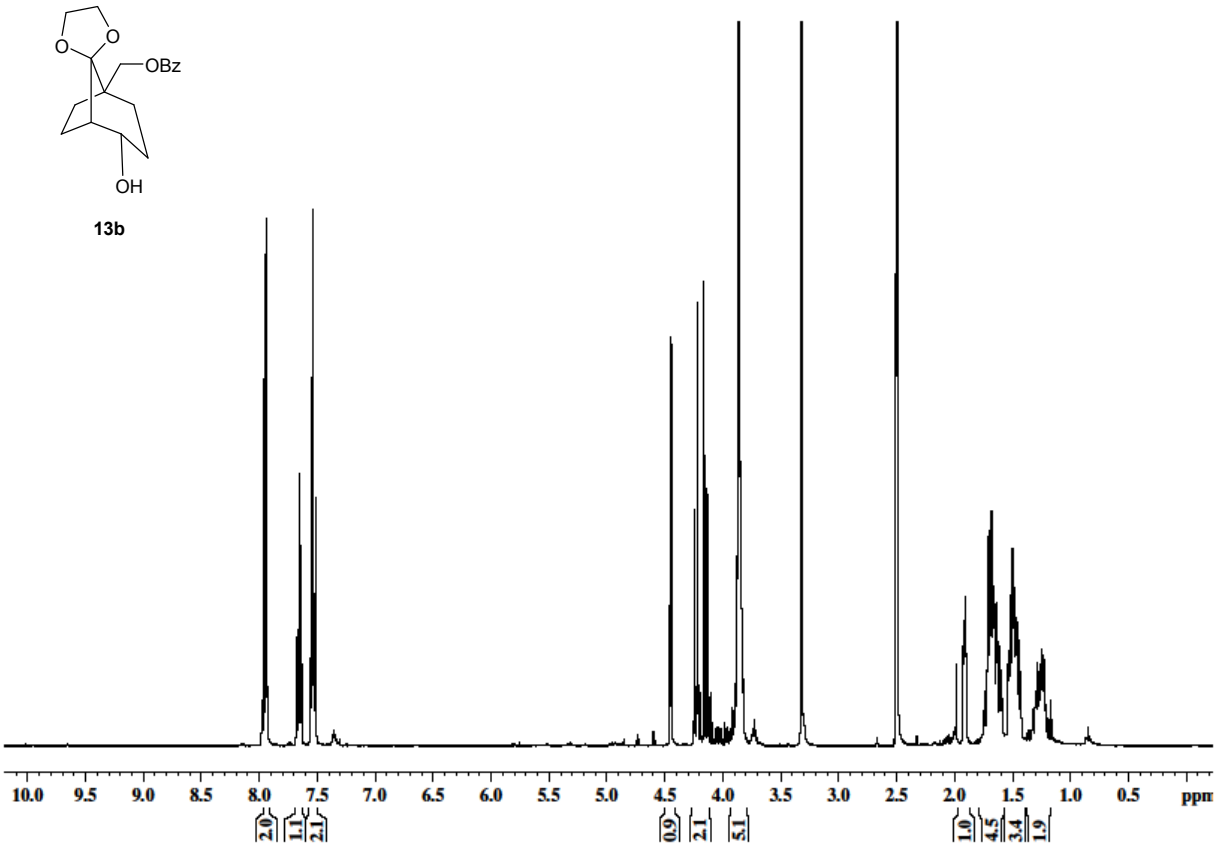
OBz
OH
13b
10.0 9.5 9.0 8.5 8.0 7.5 7.0 6.5 6.0 5.5 5.0 4.5 4.0 3.5 3.0 2.5 2.0 1.5 1.0 0.5 ppm
2.0 1.1 2.1 0.9 2.1 5.1 1.0 4.5 3.4 1.9

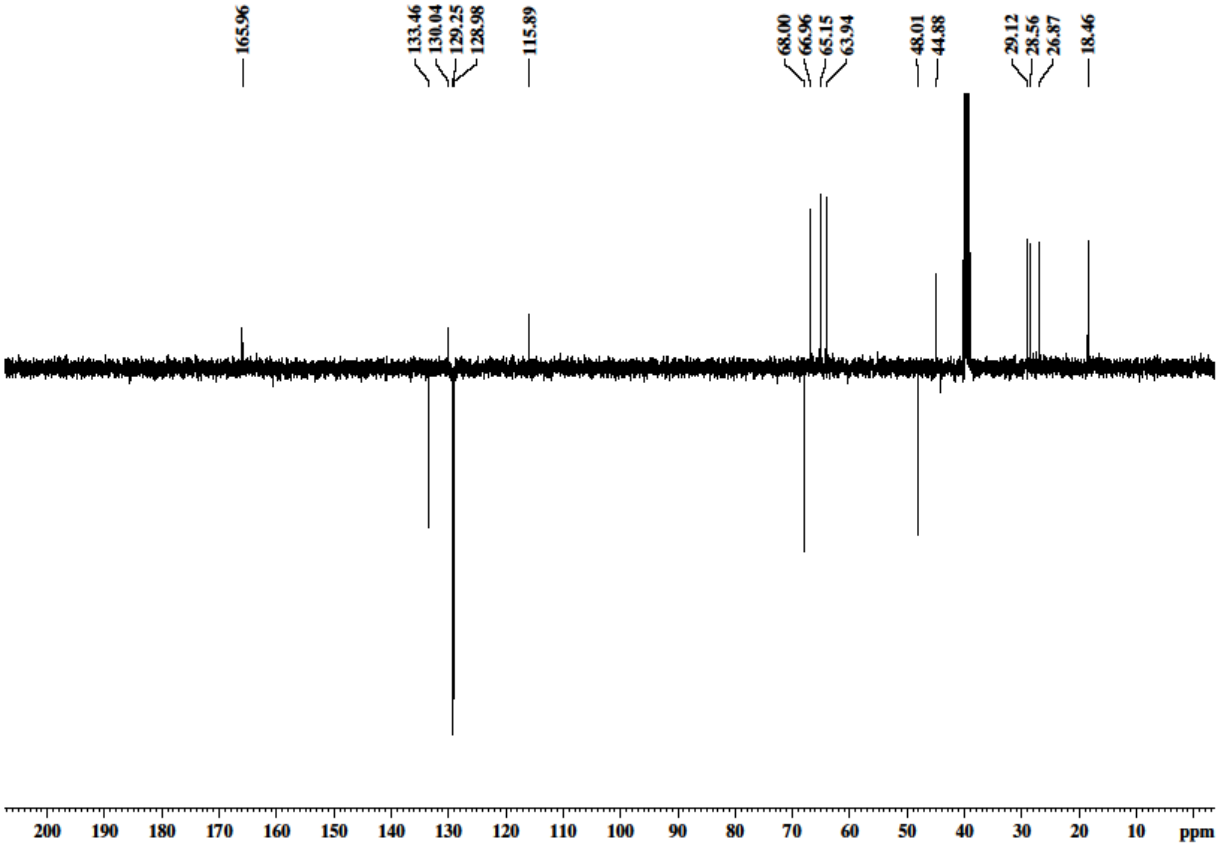
165.96
133.46
130.04
129.25
128.98
115.89
68.00
66.96
65.15
63.94
48.01
44.88
29.12
28.56
26.87
18.46
200 190 180 170 160 150 140 130 120 110 100 90 80 70 60 50 40 30 20 10 ppm

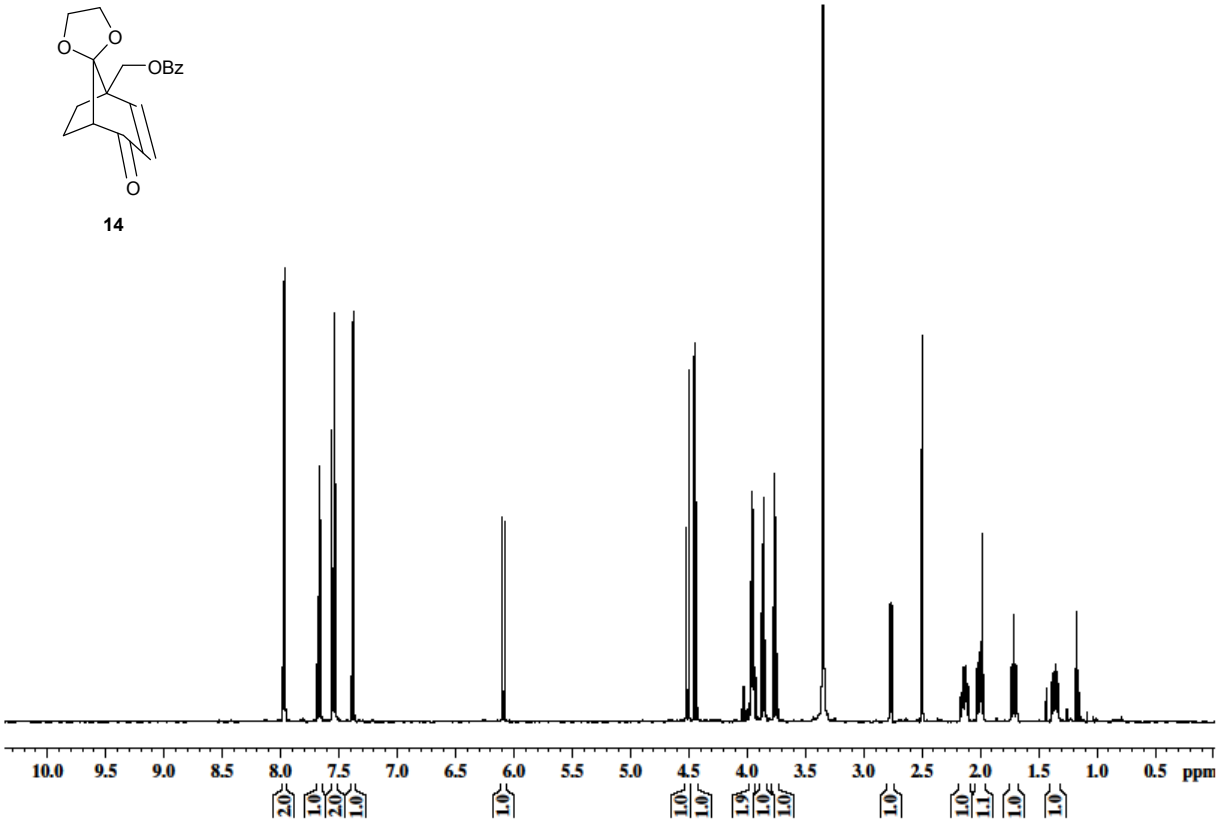
OBz
O
O
O
14
10.0 9.5 9.0 8.5 8.0 7.5 7.0 6.5 6.0 5.5 5.0 4.5 4.0 3.5 3.0 2.5 2.0 1.5 1.0 0.5 ppm
2.0 1.0 2.0 1.0 1.0 1.0 1.0 1.9 1.0 1.0 1.0 1.0 1.0 1.1 1.0 1.0

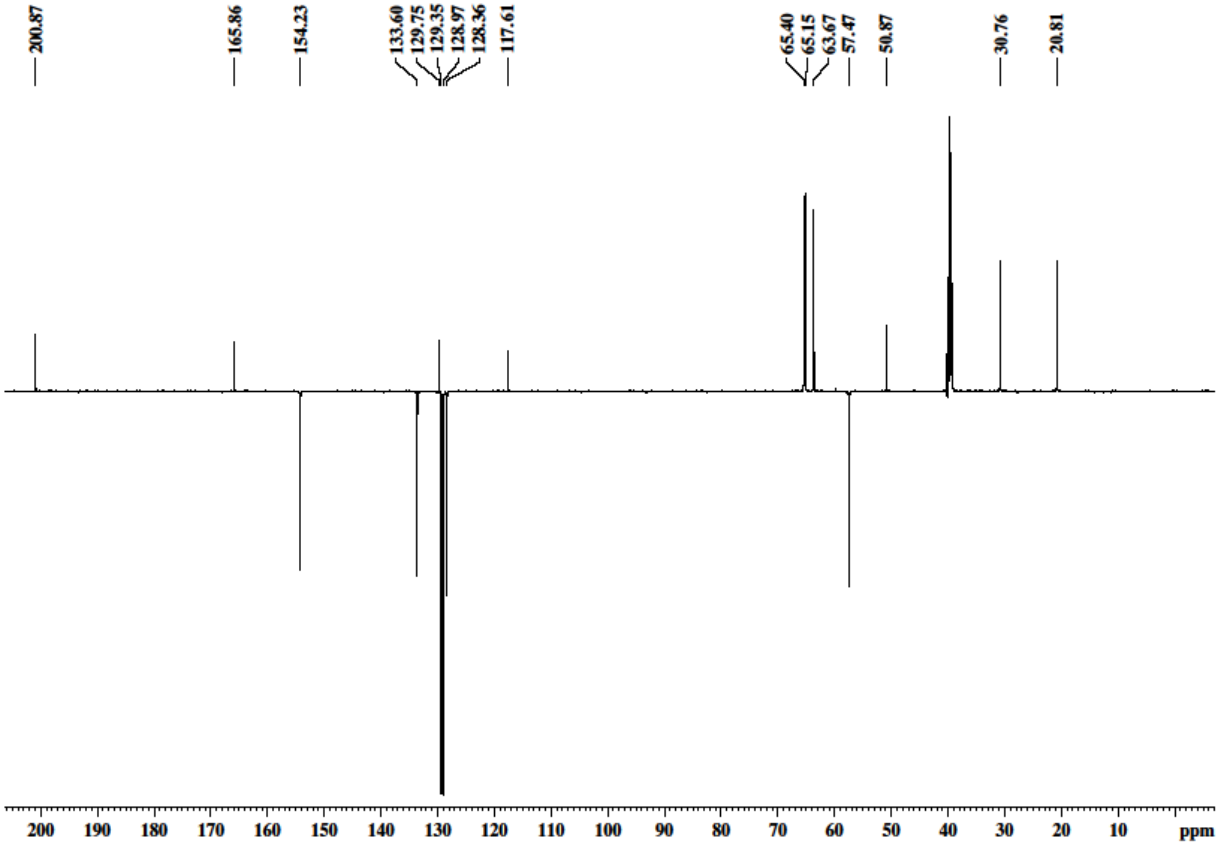
200.87
165.86
154.23
133.60
129.75
129.35
128.97
128.36
117.61
65.40
65.15
63.67
57.47
50.87
30.76
20.81
200 190 180 170 160 150 140 130 120 110 100 90 80 70 60 50 40 30 20 10 ppm

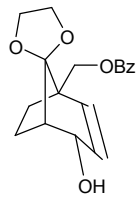
O
O
OBz
OH

15

10.0 9.5 9.0 8.5 8.0 7.5 7.0 6.5 6.0 5.5 5.0 4.5 4.0 3.5 3.0 2.5 2.0 1.5 1.0 0.5 ppm
2.0 1.0 2.0 1.0 1.0 1.0 1.0 1.0 1.0 3.0 1.1 1.0 1.0 1.0 1.0 1.0

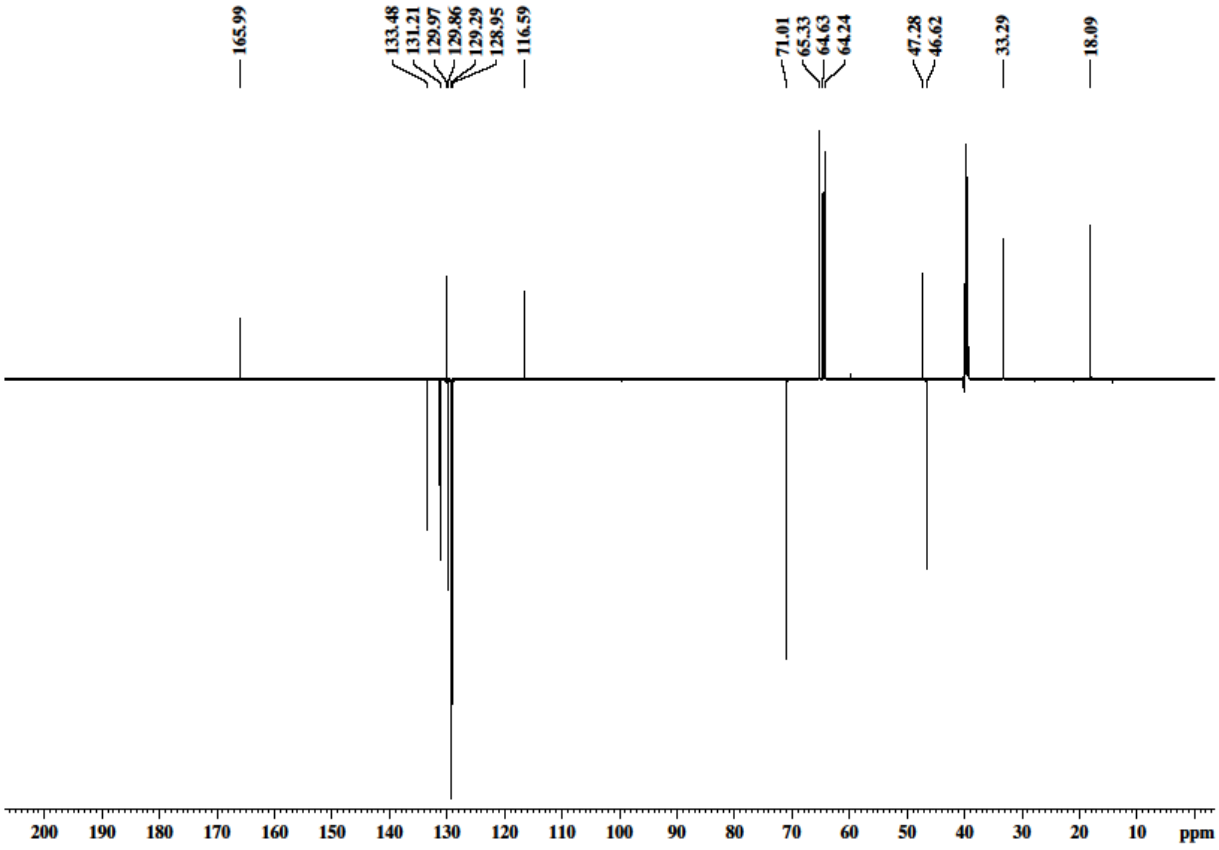
165.99
133.48
131.21
129.97
129.86
129.29
128.95
116.59
71.01
65.33
64.63
64.24
47.28
46.62
33.29
18.09
200 190 180 170 160 150 140 130 120 110 100 90 80 70 60 50 40 30 20 10 ppm

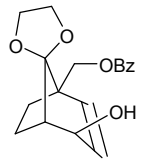
O
O
OBz
OH

16

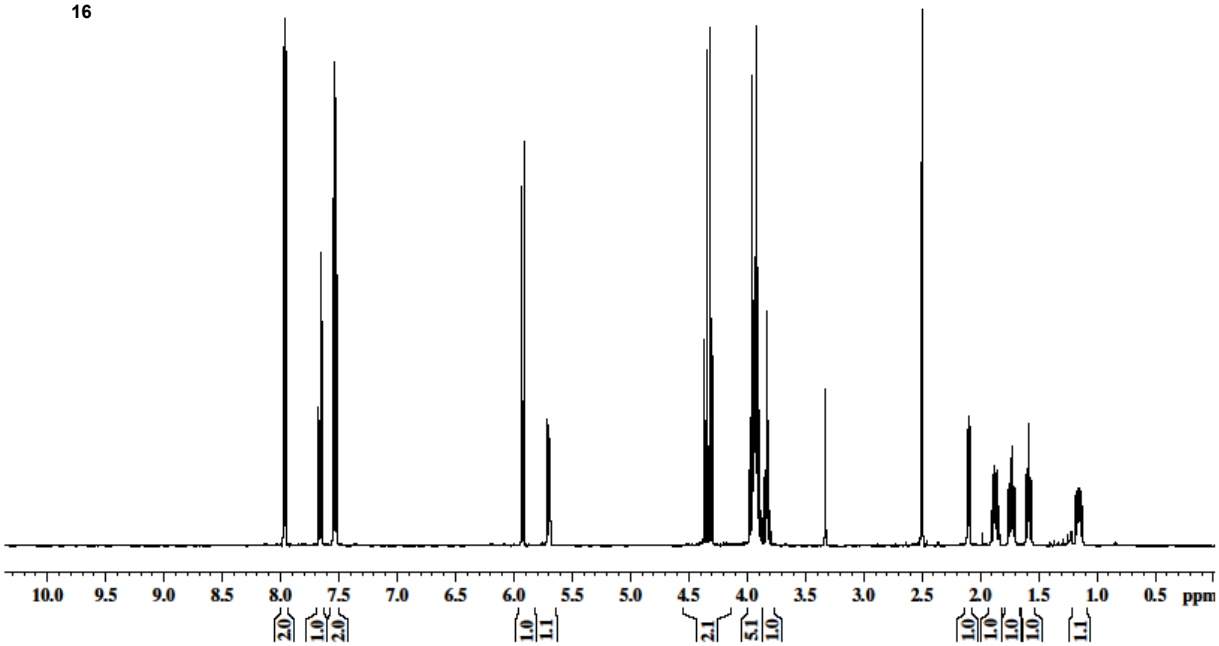
10.0 9.5 9.0 8.5 8.0 7.5 7.0 6.5 6.0 5.5 5.0 4.5 4.0 3.5 3.0 2.5 2.0 1.5 1.0 0.5 ppm
2.0 1.0 2.0 1.0 1.1 2.1 5.1 1.0 1.0 1.0 1.0 1.0 1.1

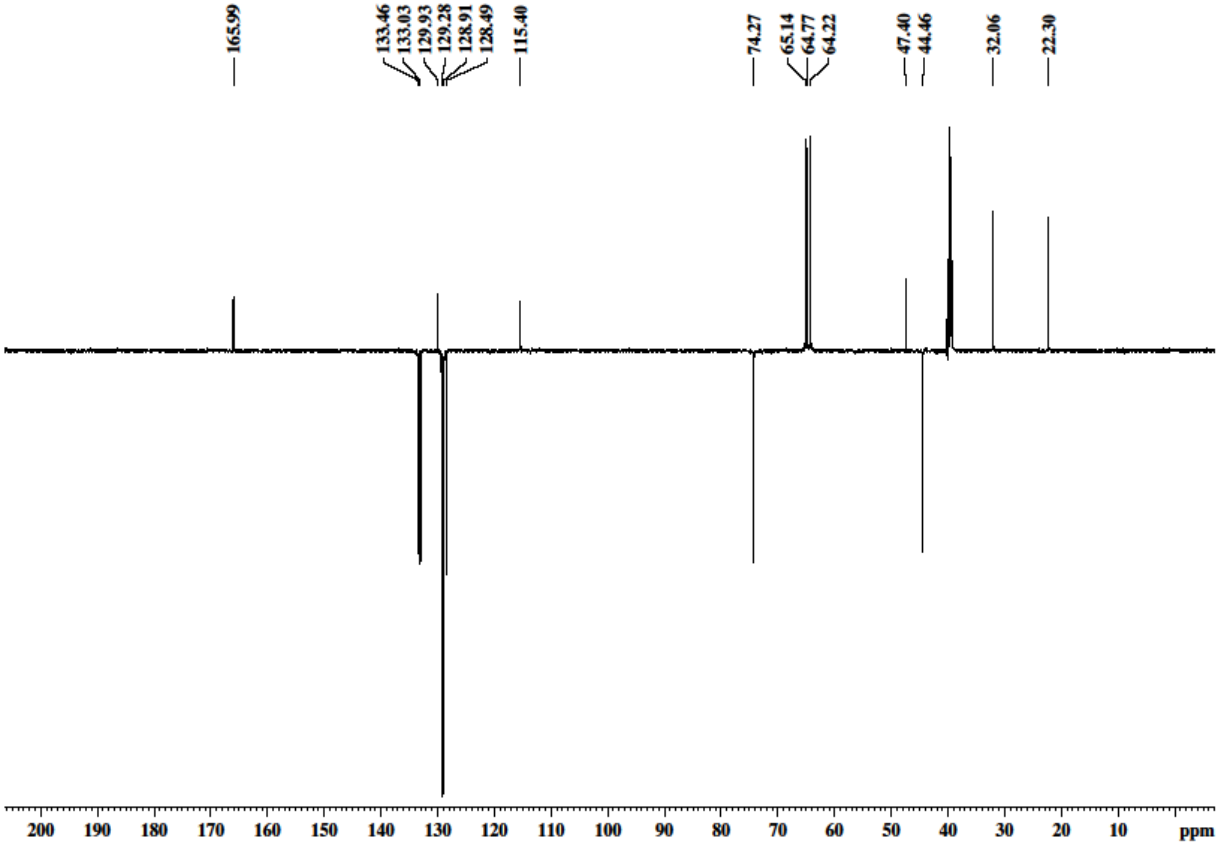
165.99
133.46
133.03
129.93
129.28
128.91
128.49
115.40
74.27
65.14
64.77
64.22
47.40
44.46
32.06
22.30
200 190 180 170 160 150 140 130 120 110 100 90 80 70 60 50 40 30 20 10 ppm

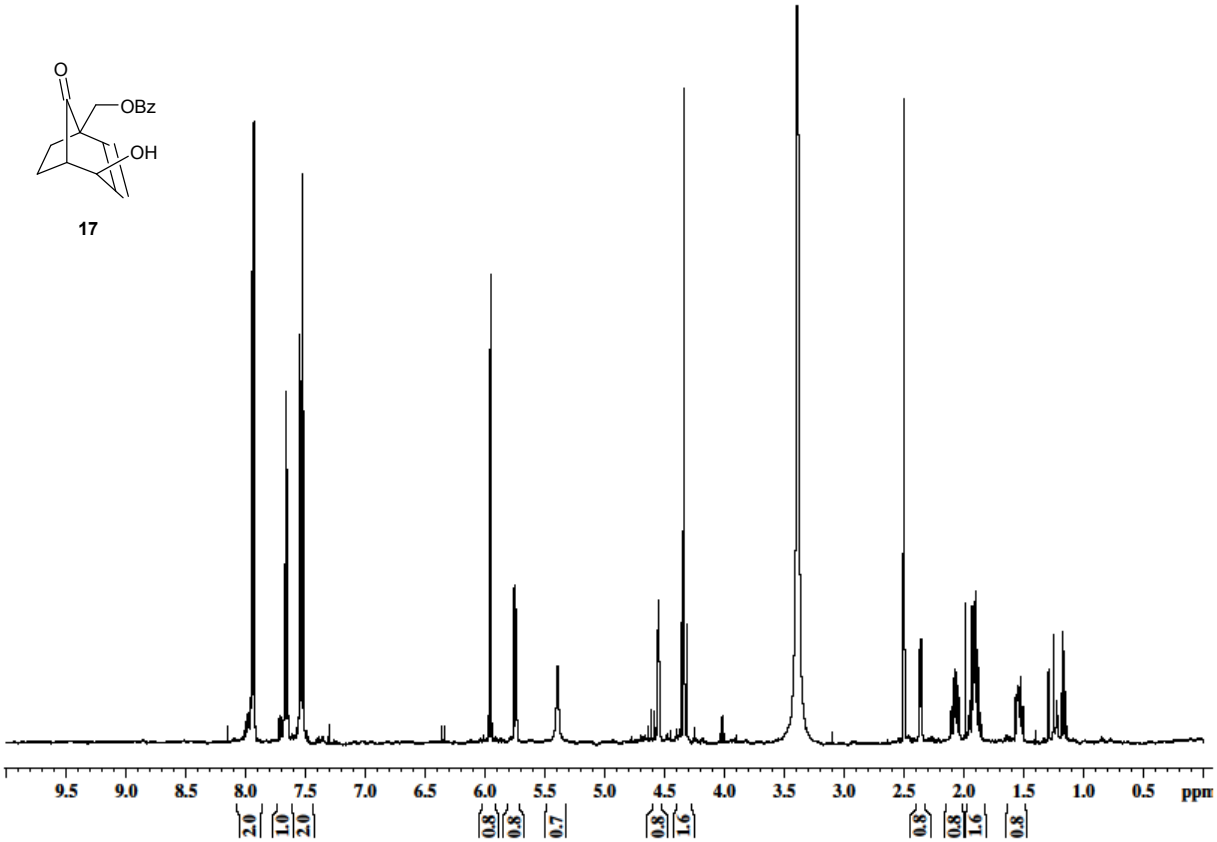
O
OBz
OH
17
9.5 9.0 8.5 8.0 7.5 7.0 6.5 6.0 5.5 5.0 4.5 4.0 3.5 3.0 2.5 2.0 1.5 1.0 0.5 ppm
2.0 1.0 2.0 0.8 0.8 0.7 0.8 1.6 0.8 0.8 1.6 0.8

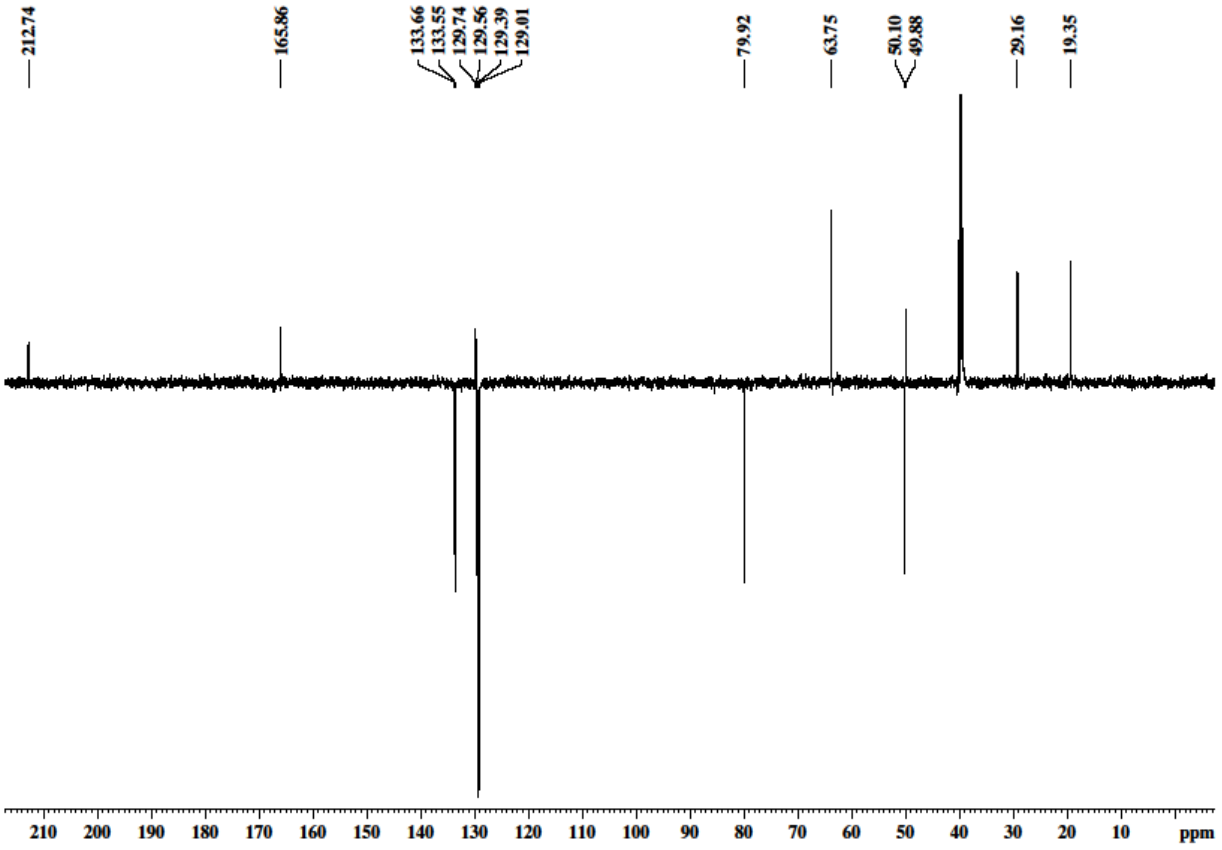
212.74
165.86
133.66
133.55
129.74
129.56
129.39
129.01
79.92
63.75
50.10
49.88
29.16
19.35
210 200 190 180 170 160 150 140 130 120 110 100 90 80 70 60 50 40 30 20 10 ppm

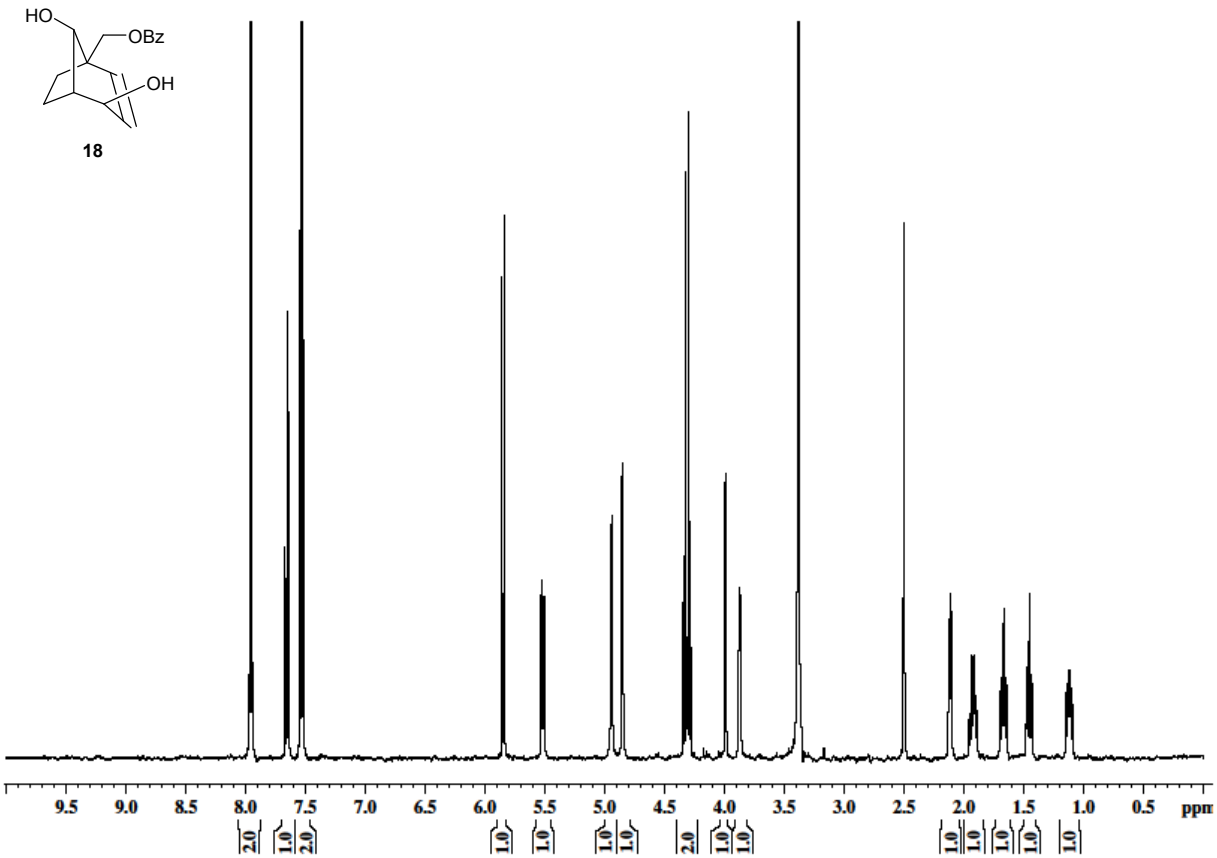
HO
OBz
OH
18
9.5 9.0 8.5 8.0 7.5 7.0 6.5 6.0 5.5 5.0 4.5 4.0 3.5 3.0 2.5 2.0 1.5 1.0 0.5 ppm
2.0 1.0 2.0 1.0 1.0 1.0 1.0 2.0 1.0 1.0 1.0 1.0 1.0 1.0 1.0 1.0

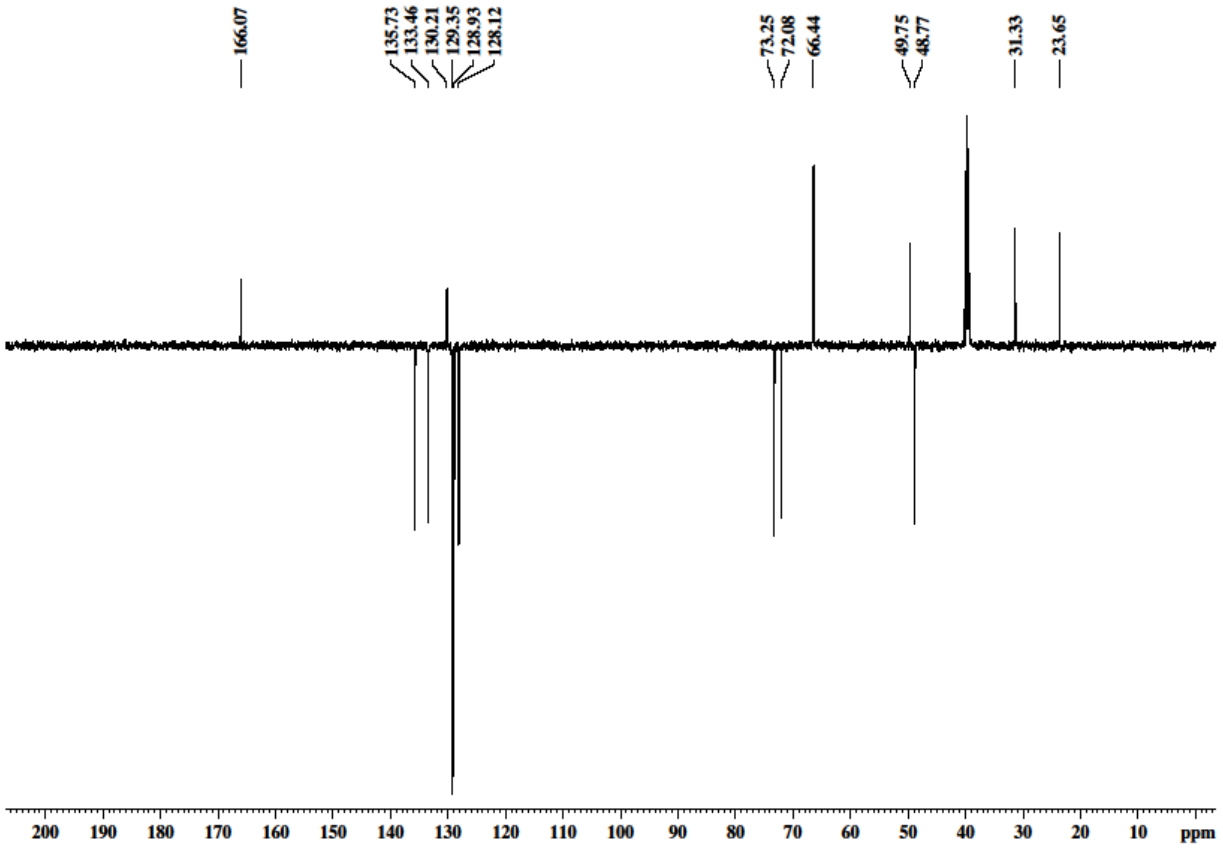
166.07
135.73
133.46
130.21
129.35
128.93
128.12
73.25
72.08
66.44
49.75
48.77
31.33
23.65
200 190 180 170 160 150 140 130 120 110 100 90 80 70 60 50 40 30 20 10 ppm

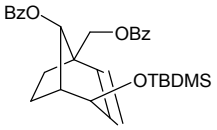
BzO
OBz
OTBDMS

19

9.5 9.0 8.5 8.0 7.5 7.0 6.5 6.0 5.5 5.0 4.5 4.0 3.5 3.0 2.5 2.0 1.5 1.0 0.5 ppm
2.1 2.1 2.0 4.1 1.0 1.0 1.0 1.0 1.1 1.1 1.0 1.0 1.1 1.1 1.0 9.2 4.6

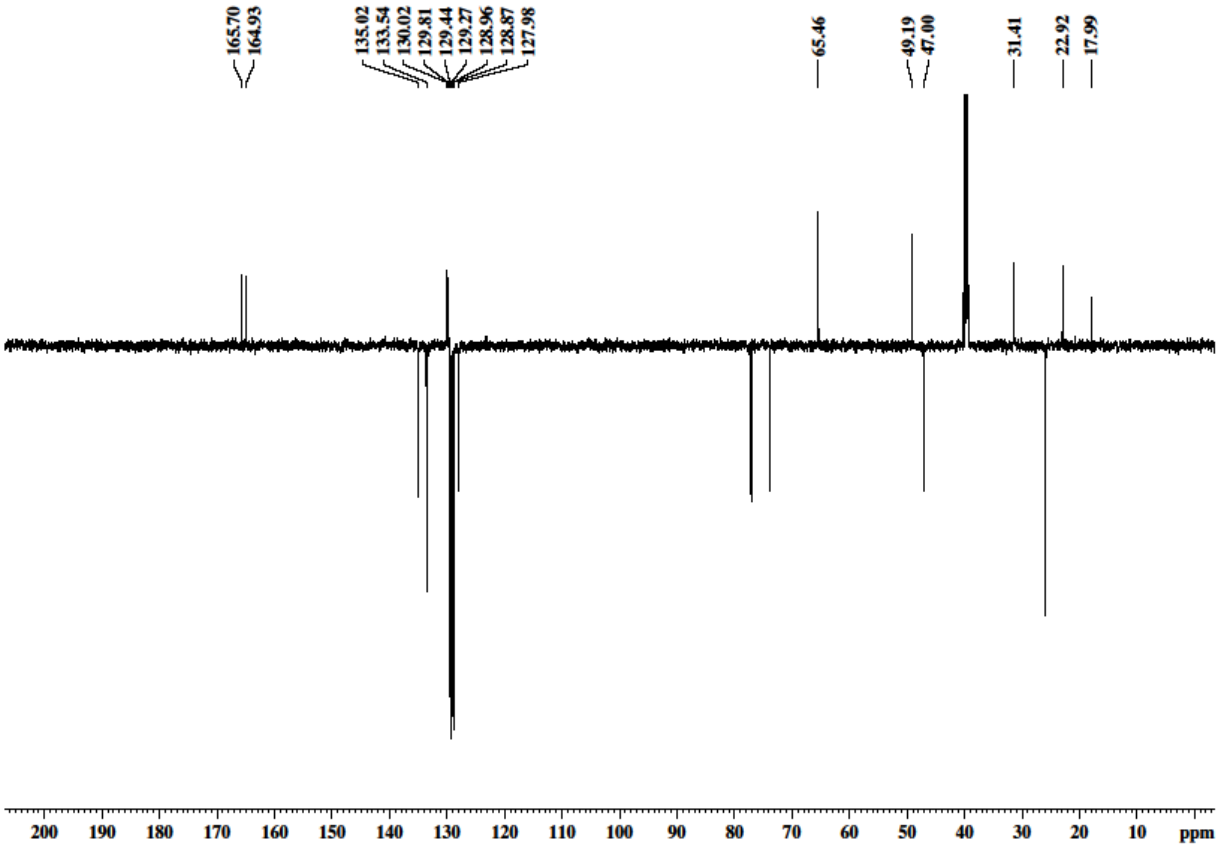
165.70
164.93
135.02
133.54
130.02
129.81
129.44
129.27
128.96
128.87
127.98
65.46
49.19
47.00
31.41
22.92
17.99
200 190 180 170 160 150 140 130 120 110 100 90 80 70 60 50 40 30 20 10 ppm

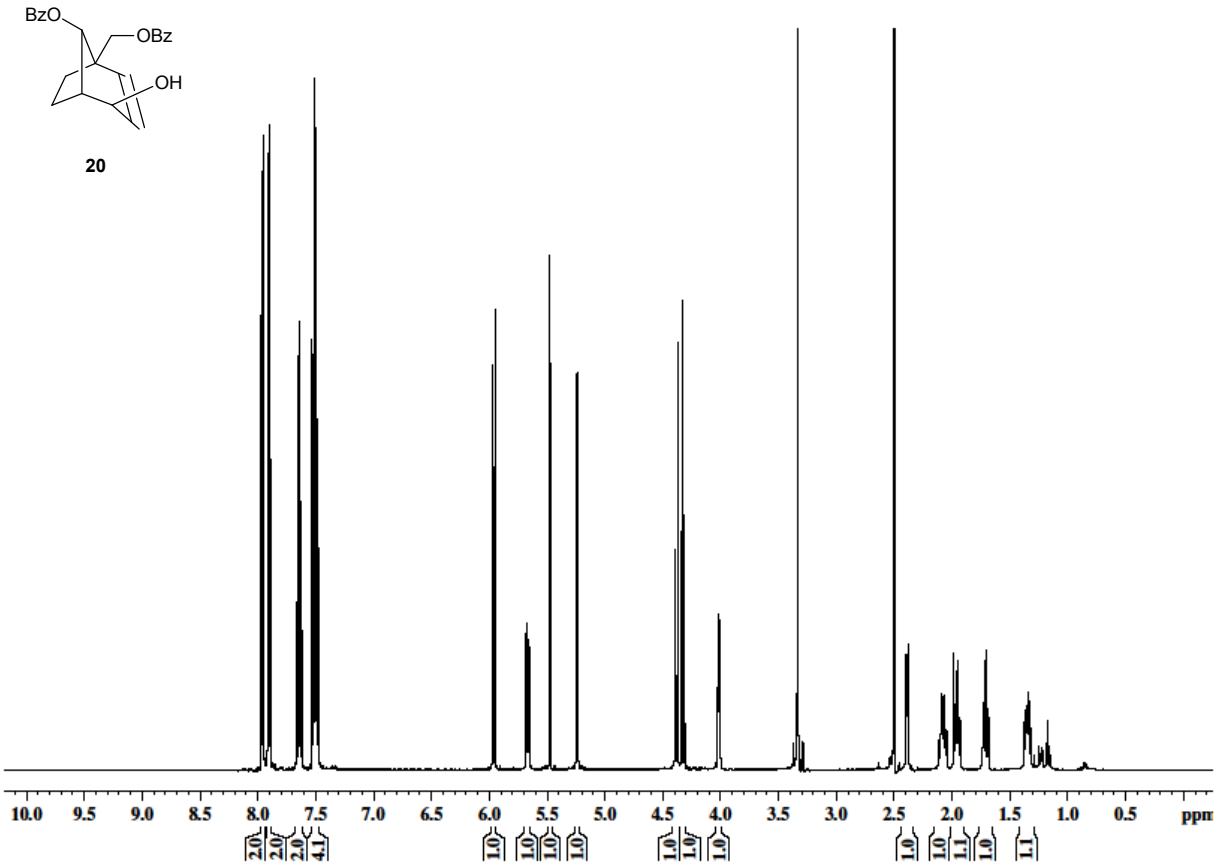
BzO
OBz
OH
20
10.0 9.5 9.0 8.5 8.0 7.5 7.0 6.5 6.0 5.5 5.0 4.5 4.0 3.5 3.0 2.5 2.0 1.5 1.0 0.5 ppm
2.0 2.0 2.0 4.1 1.0 1.0 1.0 1.0 1.0 1.0 1.0 1.0 1.0 1.1 1.0 1.1

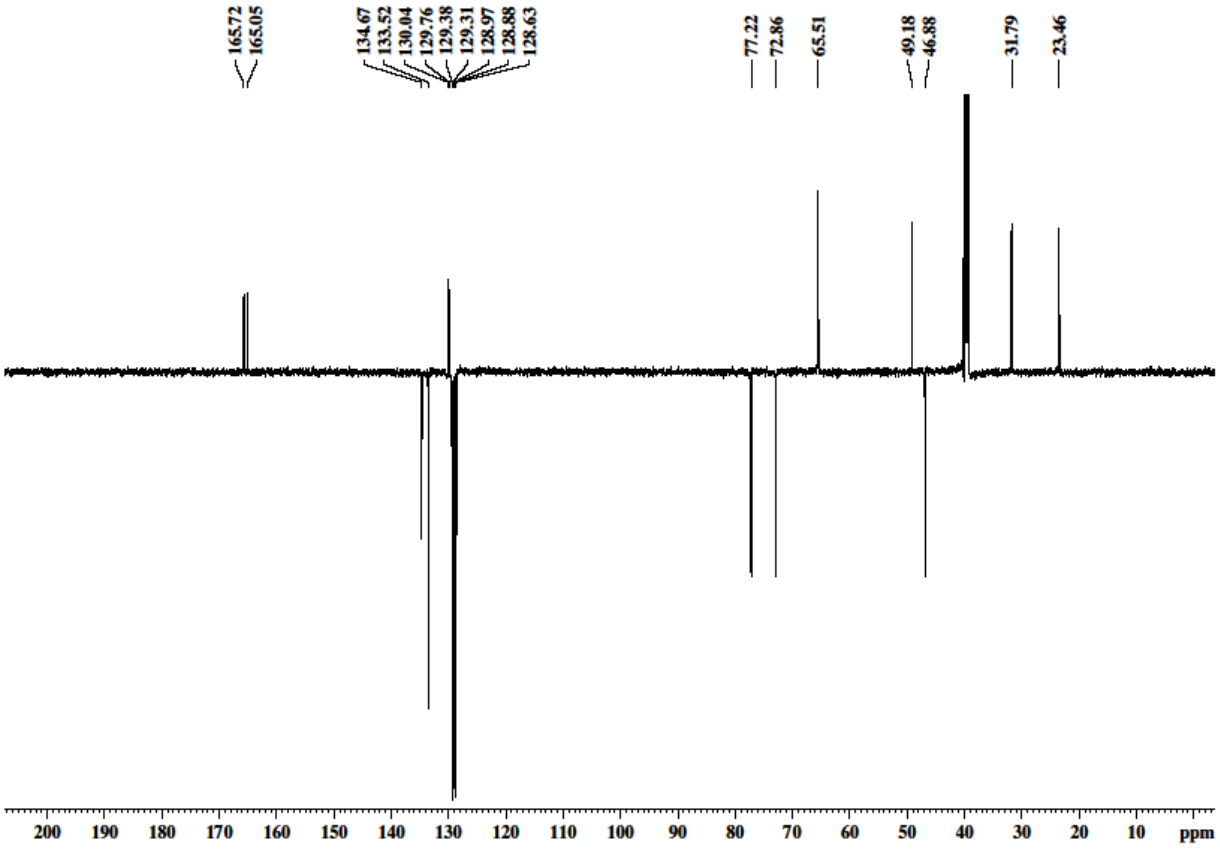
165.72
165.05
134.67
133.52
130.04
129.76
129.38
129.31
128.97
128.88
128.63
77.22
72.86
65.51
49.18
46.88
31.79
23.46
200 190 180 170 160 150 140 130 120 110 100 90 80 70 60 50 40 30 20 10 ppm

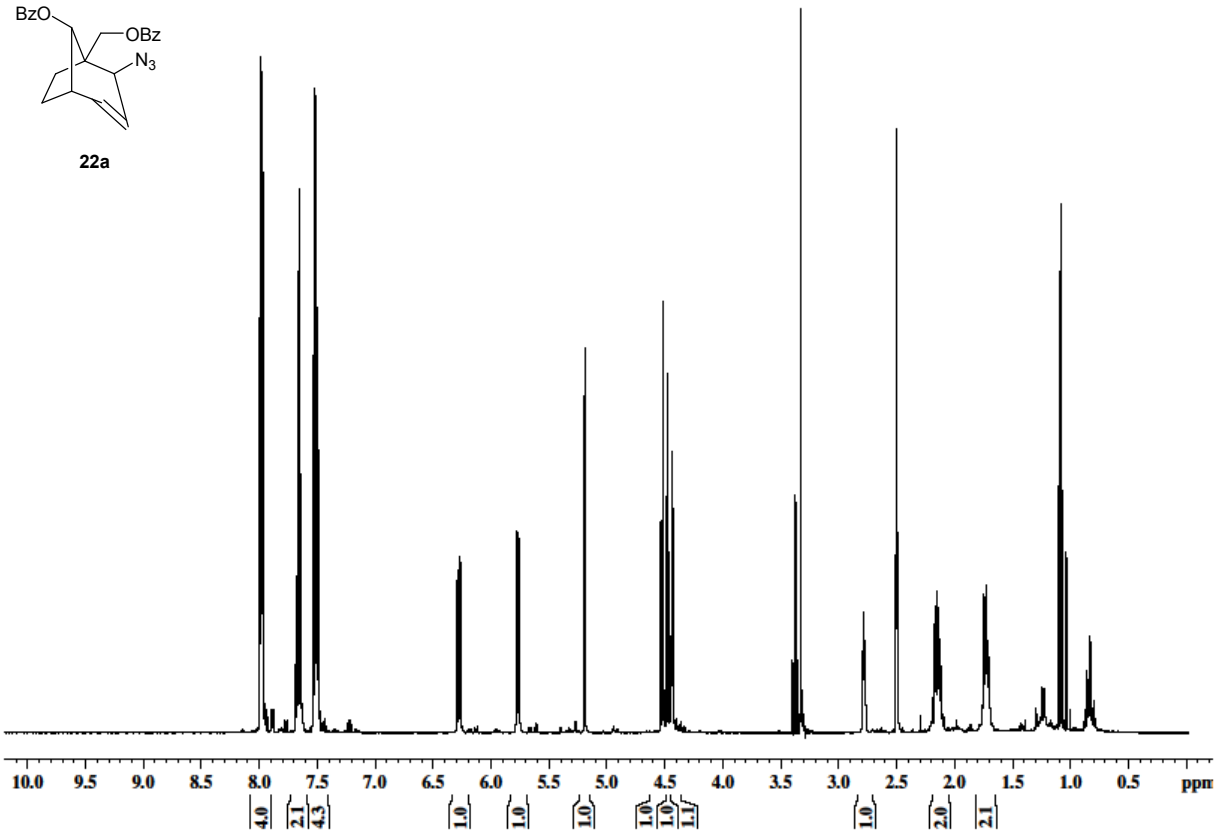
BzO
OBz
N3
22a
10.0 9.5 9.0 8.5 8.0 7.5 7.0 6.5 6.0 5.5 5.0 4.5 4.0 3.5 3.0 2.5 2.0 1.5 1.0 0.5 ppm
4.0 2.1 4.3 1.0 1.0 1.0 1.0 1.0 1.1 1.0 2.0 2.1

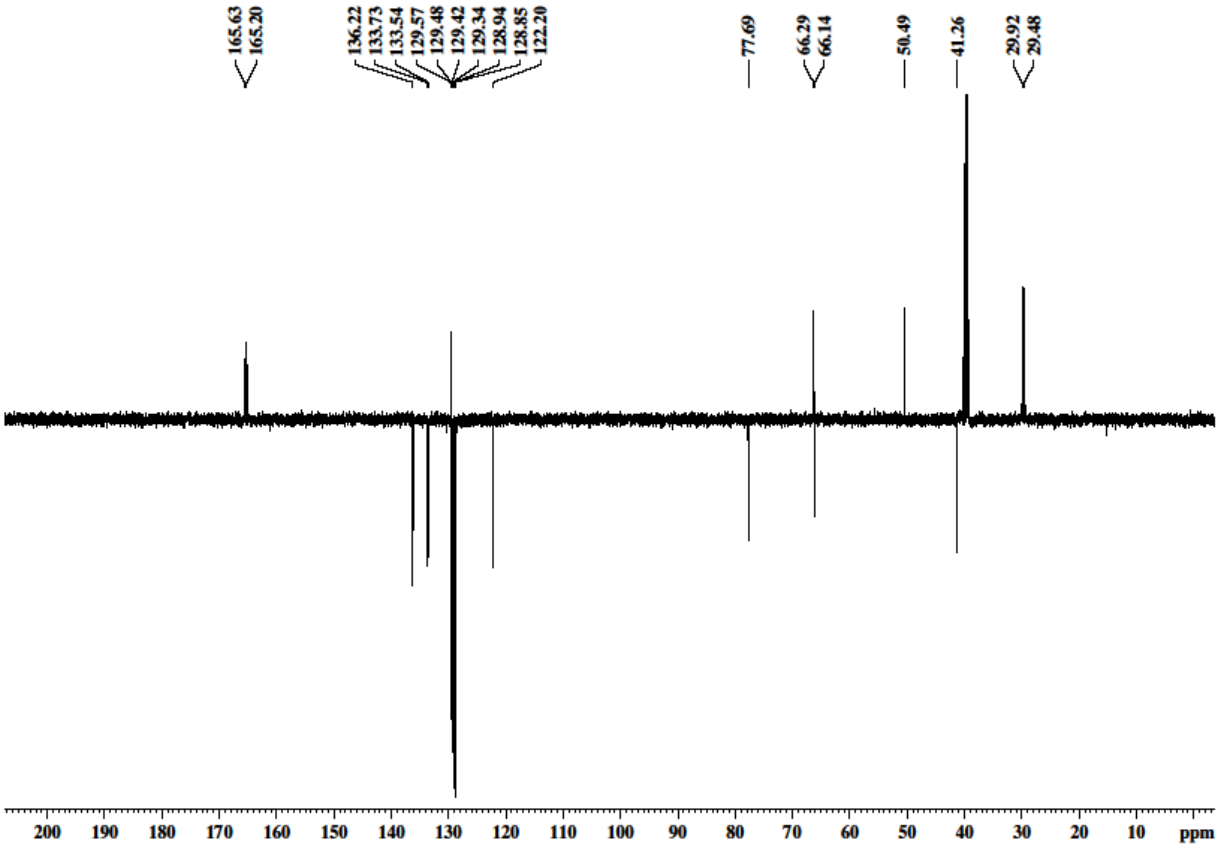
165.63
165.20
136.22
133.73
133.54
129.57
129.48
129.42
129.34
128.94
128.85
122.20
77.69
66.29
66.14
50.49
41.26
29.92
29.48
200 190 180 170 160 150 140 130 120 110 100 90 80 70 60 50 40 30 20 10 ppm

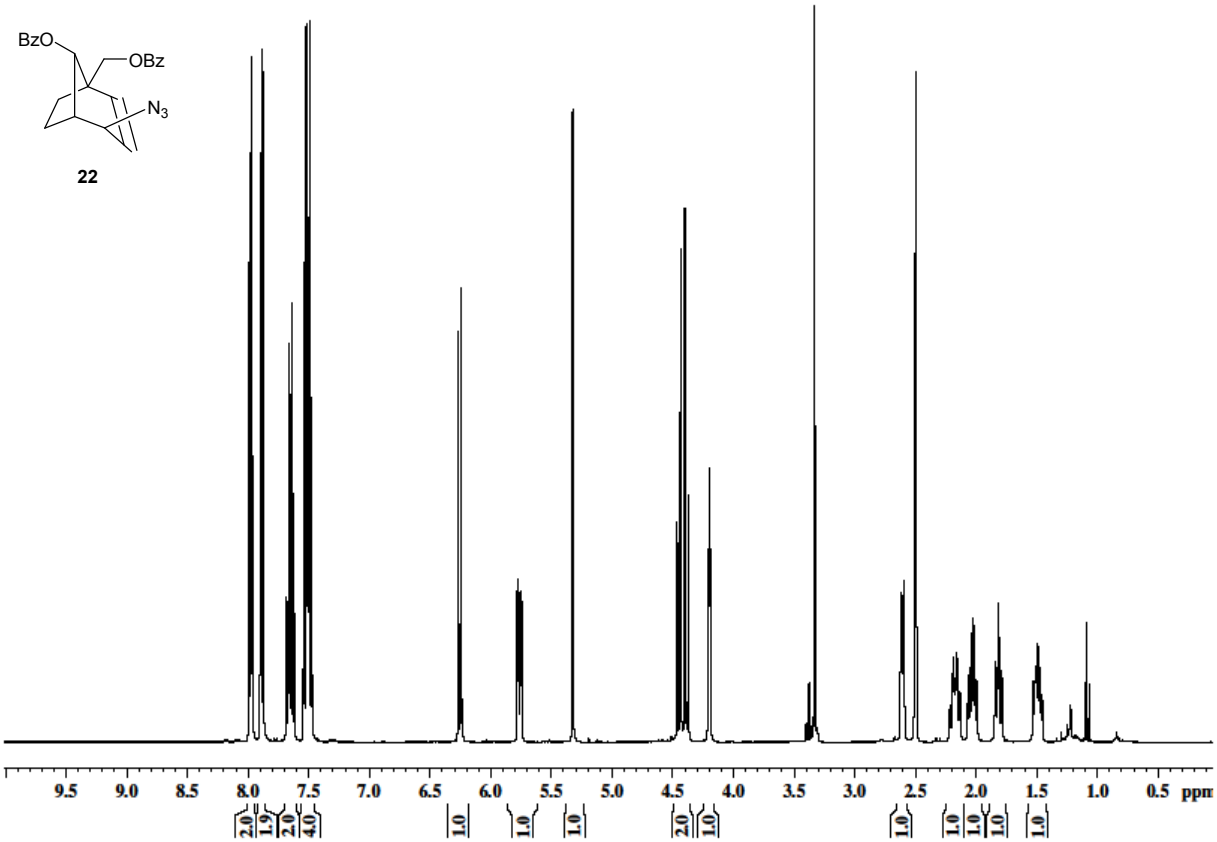
BzO
OBz
N3
22
9.5 9.0 8.5 8.0 7.5 7.0 6.5 6.0 5.5 5.0 4.5 4.0 3.5 3.0 2.5 2.0 1.5 1.0 0.5 ppm
2.0 1.9 2.0 4.0 1.0 1.0 1.0 2.0 1.0 1.0 1.0 1.0 1.0

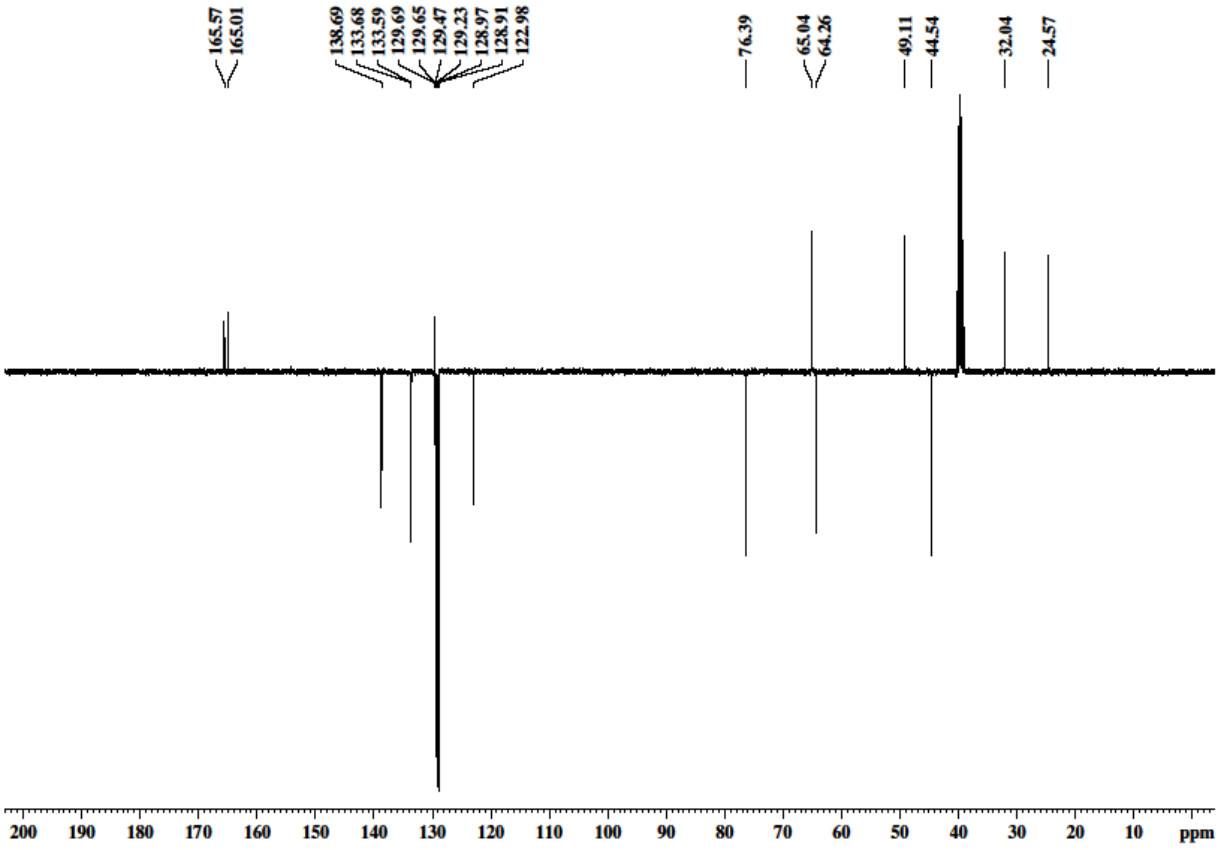
165.57
165.01
138.69
133.68
133.59
129.69
129.65
129.47
129.23
128.97
128.91
122.98
76.39
65.04
64.26
49.11
44.54
32.04
24.57
200 190 180 170 160 150 140 130 120 110 100 90 80 70 60 50 40 30 20 10 ppm

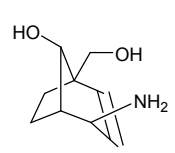
HO
OH
NH2

x HCl

23

9.5 9.0 8.5 8.0 7.5 7.0 6.5 6.0 5.5 5.0 4.5 4.0 3.5 3.0 2.5 2.0 1.5 1.0 0.5 ppm
2.9
1.0
1.0
1.6
1.0
2.2
1.9
1.0
1.0
1.0
1.0
1.1

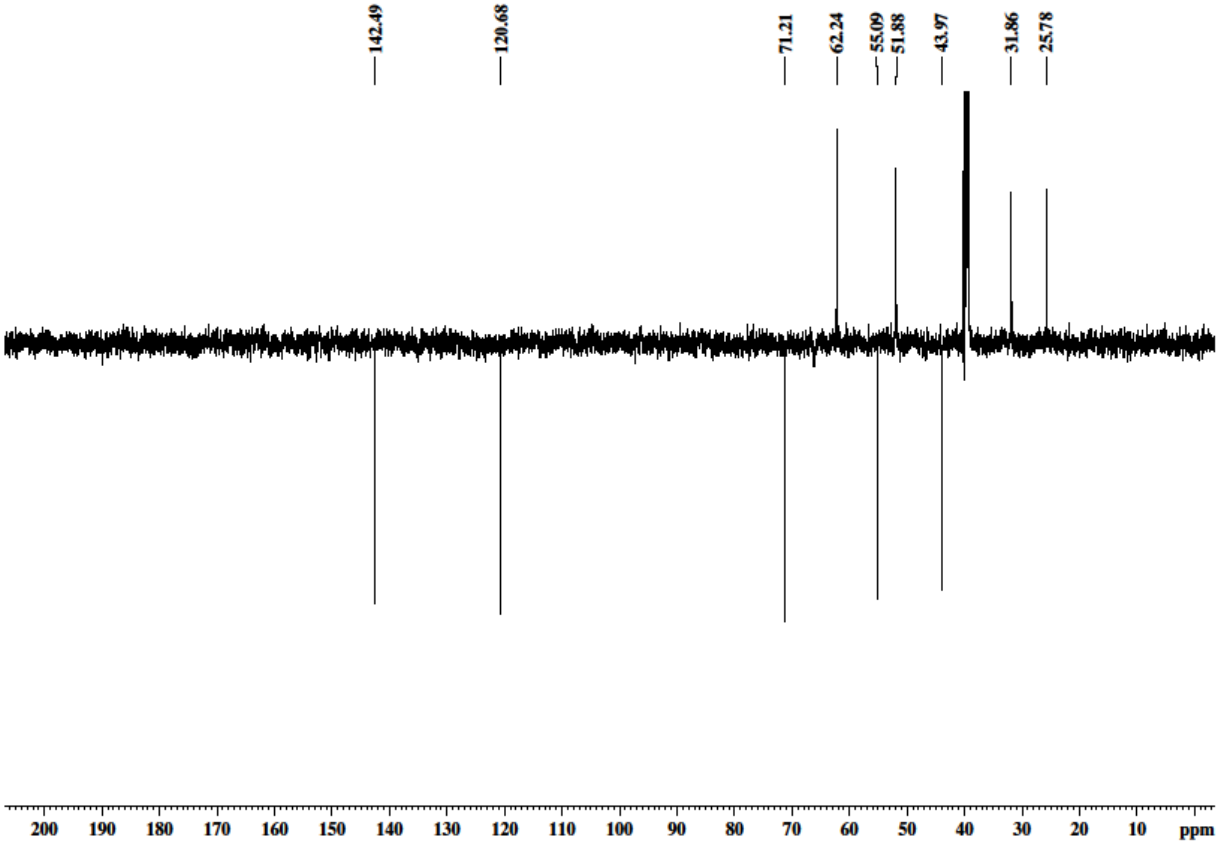
142.49
120.68
71.21
62.24
55.09
51.88
43.97
31.86
25.78
200 190 180 170 160 150 140 130 120 110 100 90 80 70 60 50 40 30 20 10 ppm

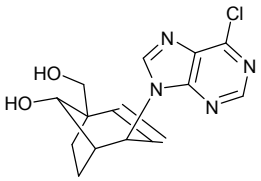
Cl
N
N
N
N
HO
HO

24

9.5 9.0 8.5 8.0 7.5 7.0 6.5 6.0 5.5 5.0 4.5 4.0 3.5 3.0 2.5 2.0 1.5 1.0 0.5 ppm
0.9 1.0 1.0 1.0 1.0 1.0 1.0 1.0 1.0 1.0 1.0 1.0 1.0

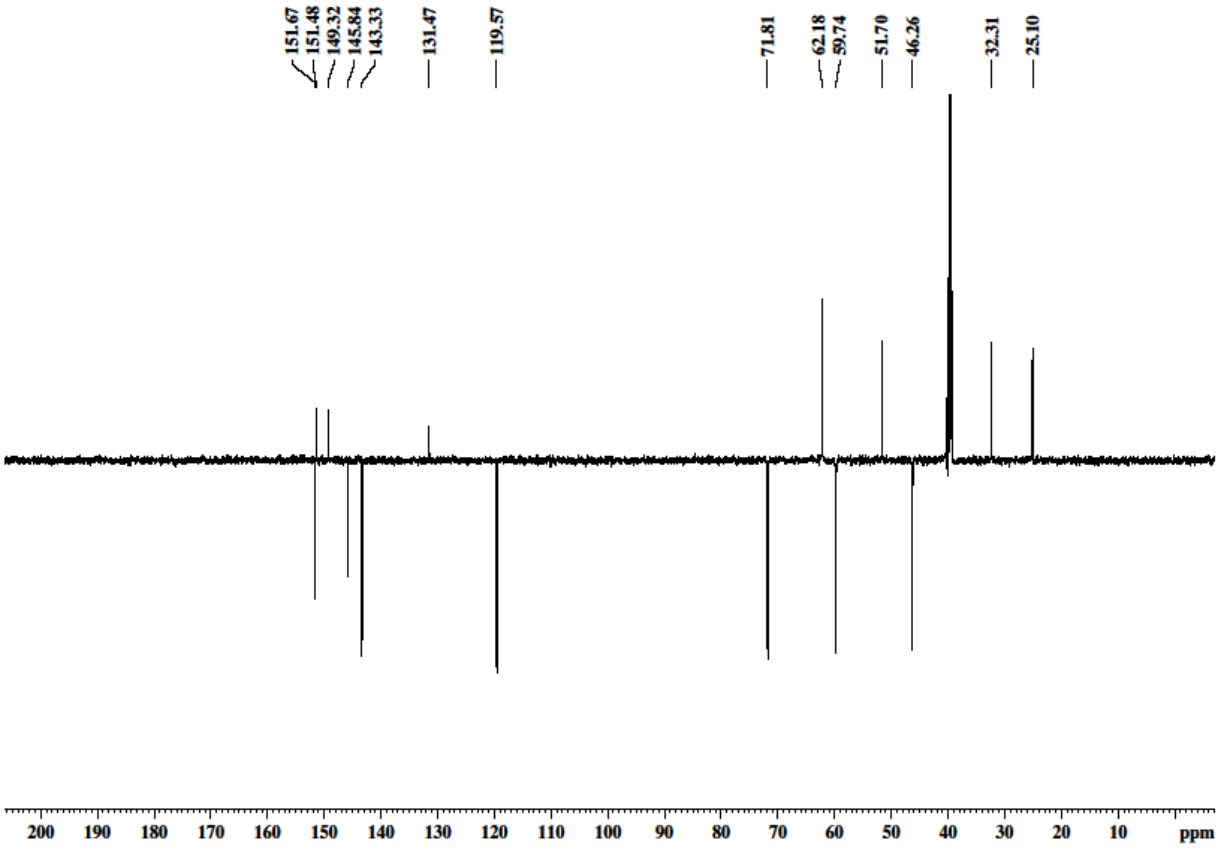
151.67
151.48
149.32
145.84
143.33
131.47
119.57
71.81
62.18
59.74
51.70
46.26
32.31
25.10
200 190 180 170 160 150 140 130 120 110 100 90 80 70 60 50 40 30 20 10 ppm

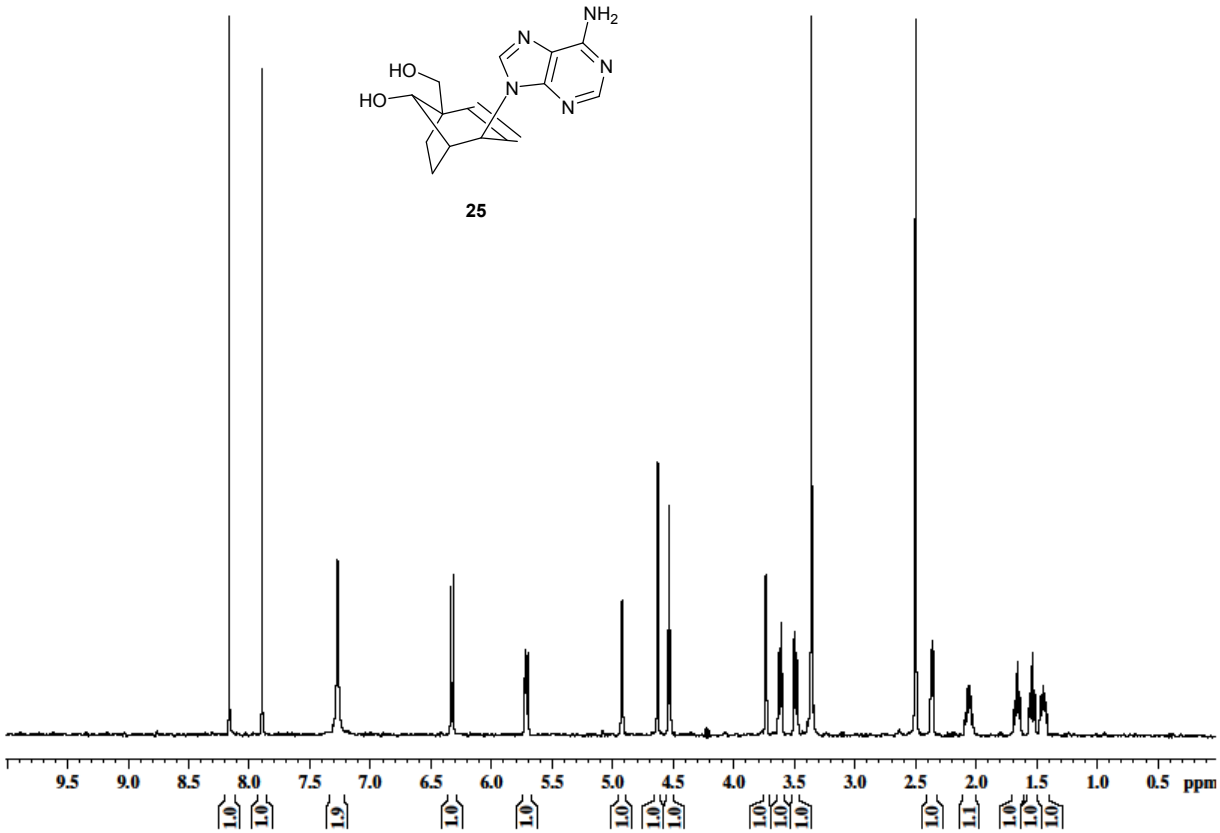
NH2
N
N
N
N
HO
HO
9.5 9.0 8.5 8.0 7.5 7.0 6.5 6.0 5.5 5.0 4.5 4.0 3.5 3.0 2.5 2.0 1.5 1.0 0.5 ppm
1.0 1.0 1.9 1.0 1.0 1.0 1.0 1.0 1.0 1.0 1.0 1.0 1.0 1.1 1.0 1.0 1.0

25

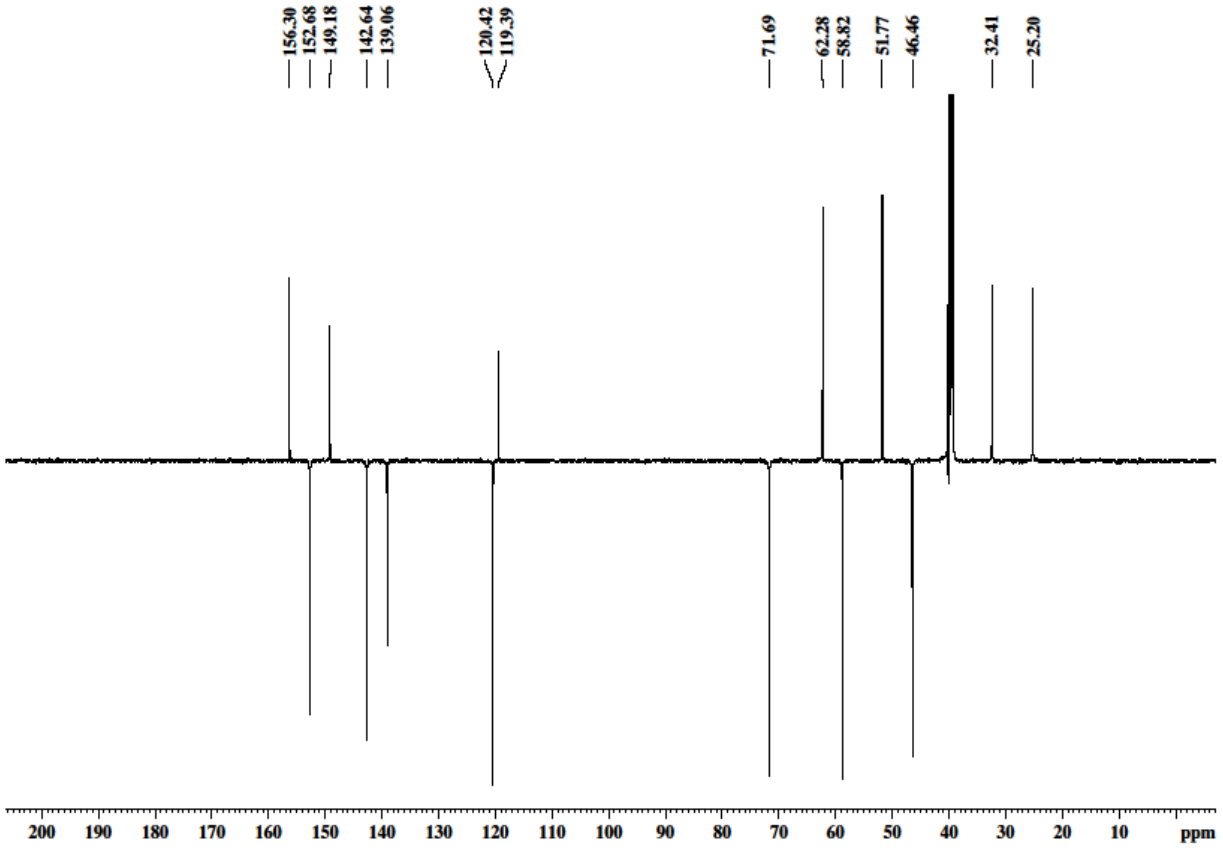
156.30
152.68
149.18
142.64
139.06
120.42
119.39
71.69
62.28
58.82
51.77
46.46
32.41
25.20
200 190 180 170 160 150 140 130 120 110 100 90 80 70 60 50 40 30 20 10 ppm

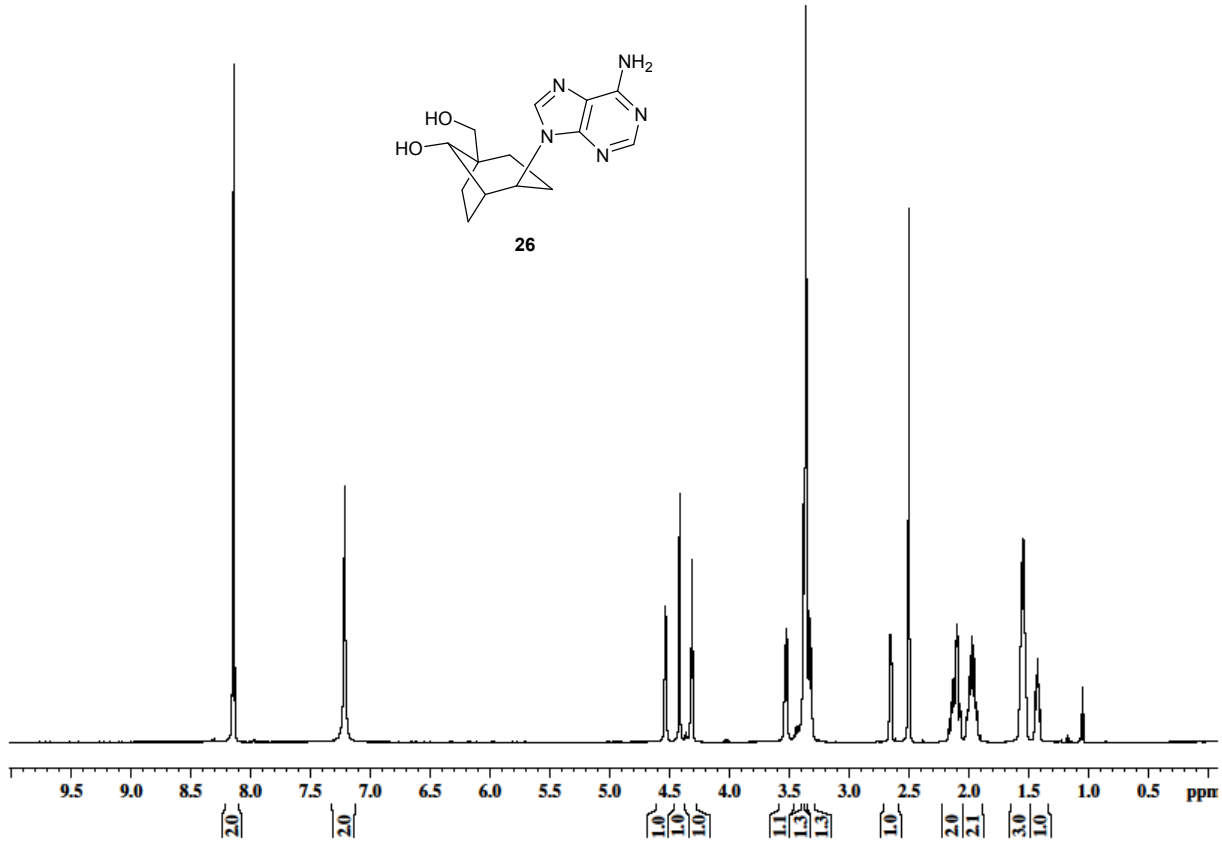
NH2
N
N
N
N
HO
HO
9.5 9.0 8.5 8.0 7.5 7.0 6.5 6.0 5.5 5.0 4.5 4.0 3.5 3.0 2.5 2.0 1.5 1.0 0.5 ppm
2.0 2.0 1.0 1.0 1.0 1.1 1.3 1.3 1.3 1.0 2.0 2.1 3.0 1.0

26

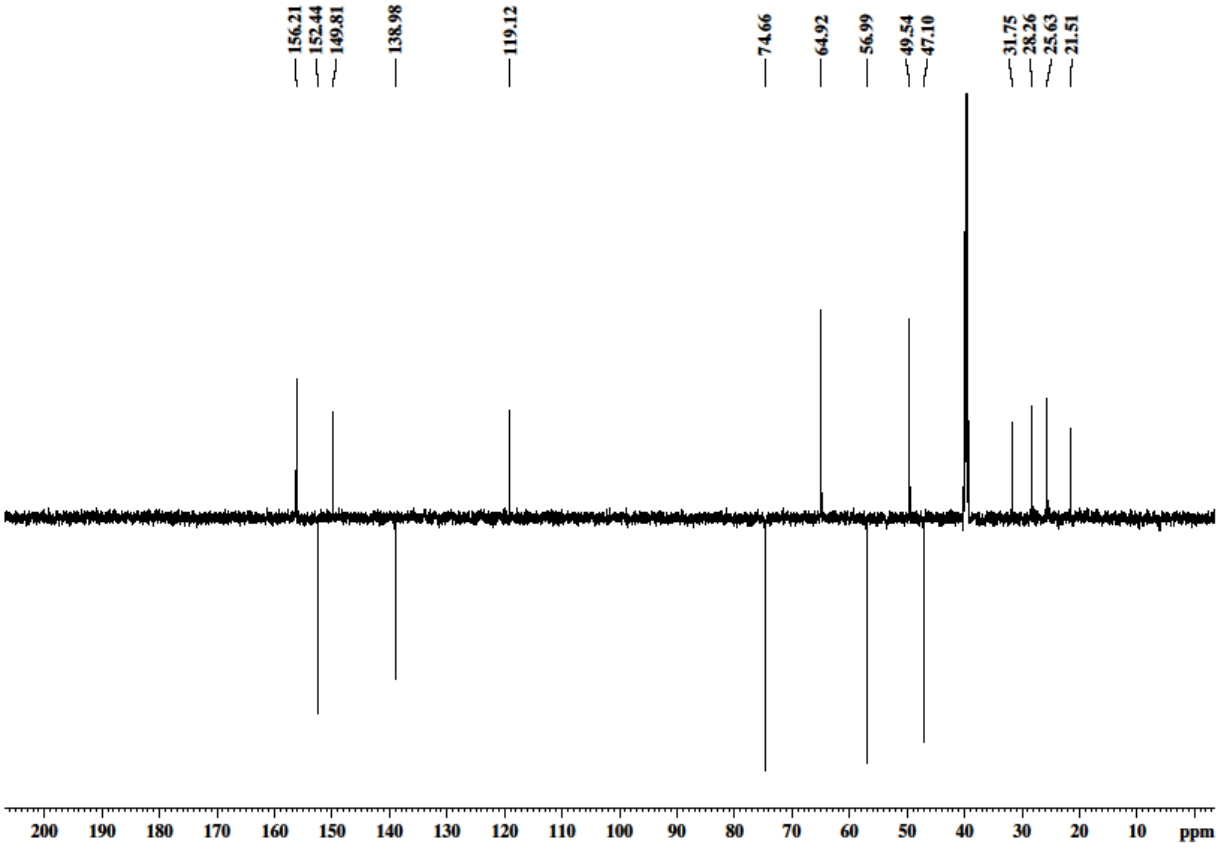
156.21
152.44
149.81
138.98
119.12
74.66
64.92
56.99
49.54
47.10
31.75
28.26
25.63
21.51
200 190 180 170 160 150 140 130 120 110 100 90 80 70 60 50 40 30 20 10 ppm

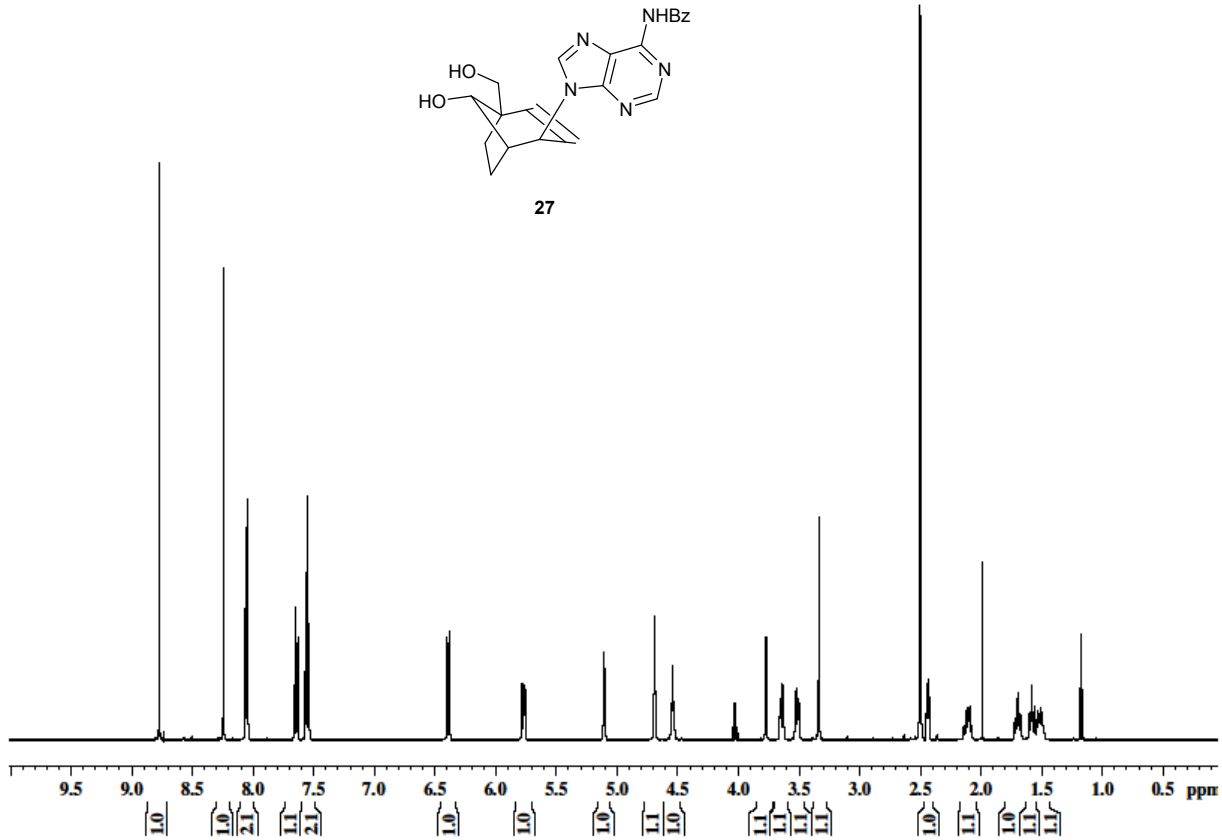
NHBz
N
N
N
N
HO
HO
9.5 9.0 8.5 8.0 7.5 7.0 6.5 6.0 5.5 5.0 4.5 4.0 3.5 3.0 2.5 2.0 1.5 1.0 0.5 ppm
1.0 1.0 2.1 1.1 2.1 1.0 1.0 1.0 1.1 1.0 1.1 1.1 1.1 1.0 1.1 1.0 1.1 1.1

27

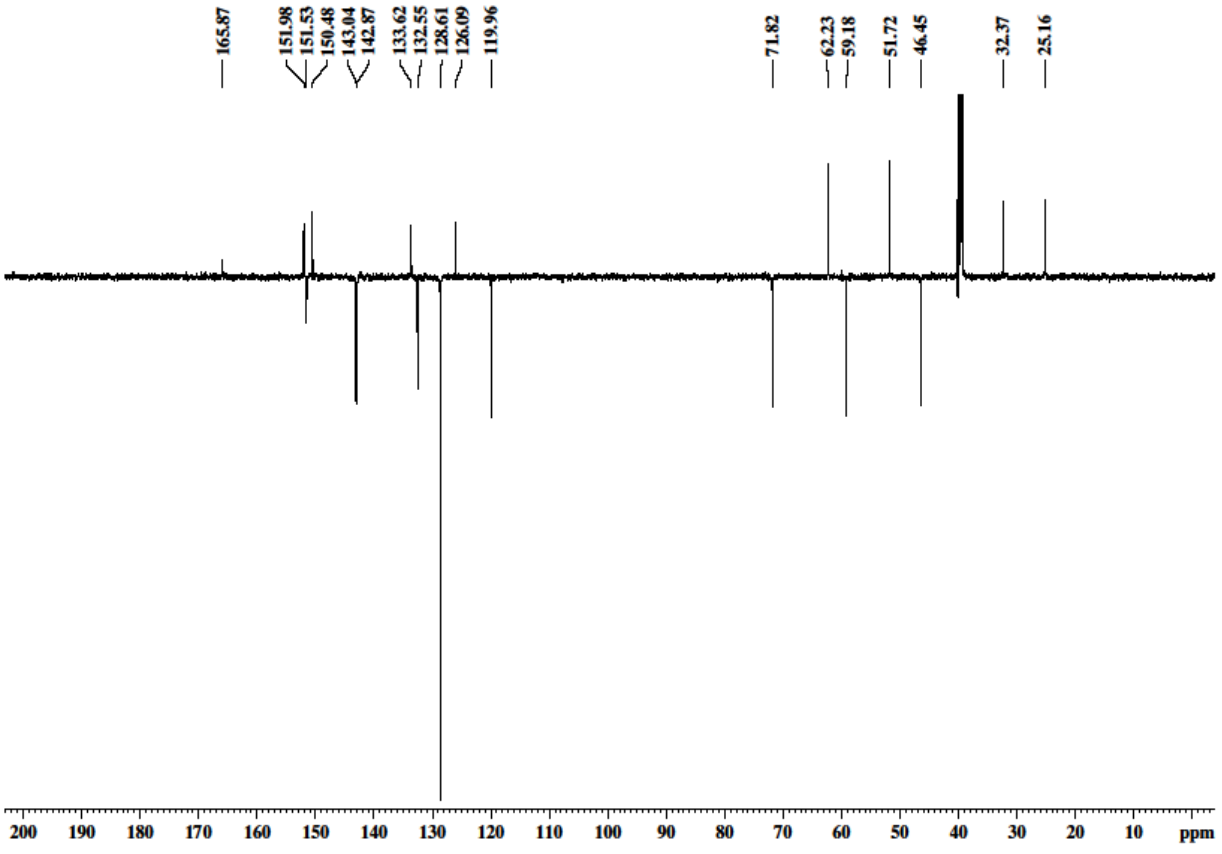
165.87
151.98
151.53
150.48
143.04
142.87
133.62
132.55
128.61
126.09
119.96
71.82
62.23
59.18
51.72
46.45
32.37
25.16
200 190 180 170 160 150 140 130 120 110 100 90 80 70 60 50 40 30 20 10 ppm

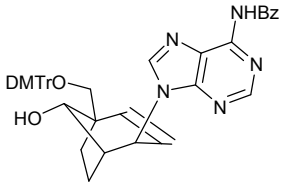
NHBz
N
N
N
N
DMTrO
HO

28

11.5 11.0 10.5 10.0 9.5 9.0 8.5 8.0 7.5 7.0 6.5 6.0 5.5 5.0 4.5 4.0 3.5 3.0 2.5 2.0 1.5 1.0 0.5 ppm
0.4 1.0 1.0 2.1 1.1 2.1 2.2 2.6 4.0 1.2 4.4 0.9 0.9 0.8 0.8 1.1 6.6 1.3 1.1 1.0 2.1 1.0

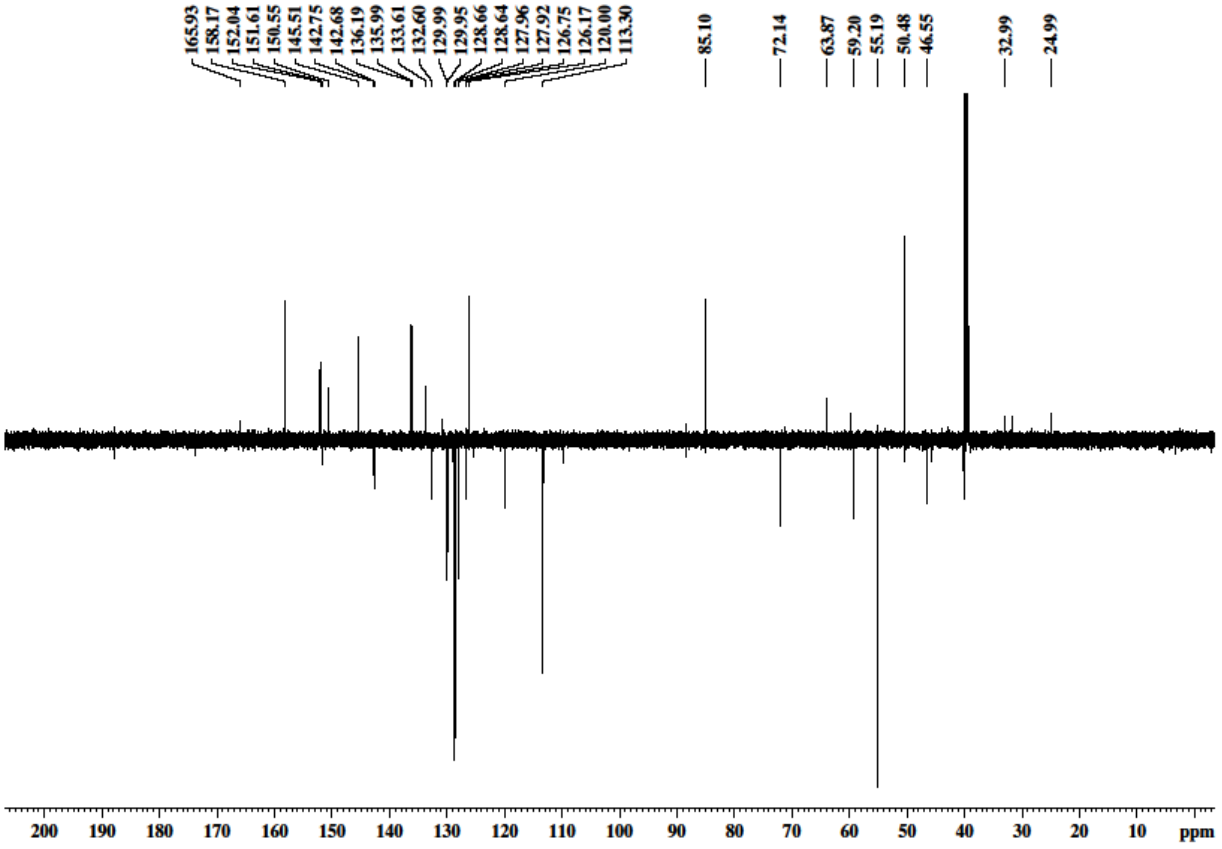
165.93
158.17
152.04
151.61
150.55
145.51
142.75
142.68
136.19
135.99
133.61
132.60
129.99
129.95
128.66
128.64
127.96
127.92
126.75
126.17
120.00
113.30
85.10
72.14
63.87
59.20
55.19
50.48
46.55
32.99
24.99
200 190 180 170 160 150 140 130 120 110 100 90 80 70 60 50 40 30 20 10 ppm

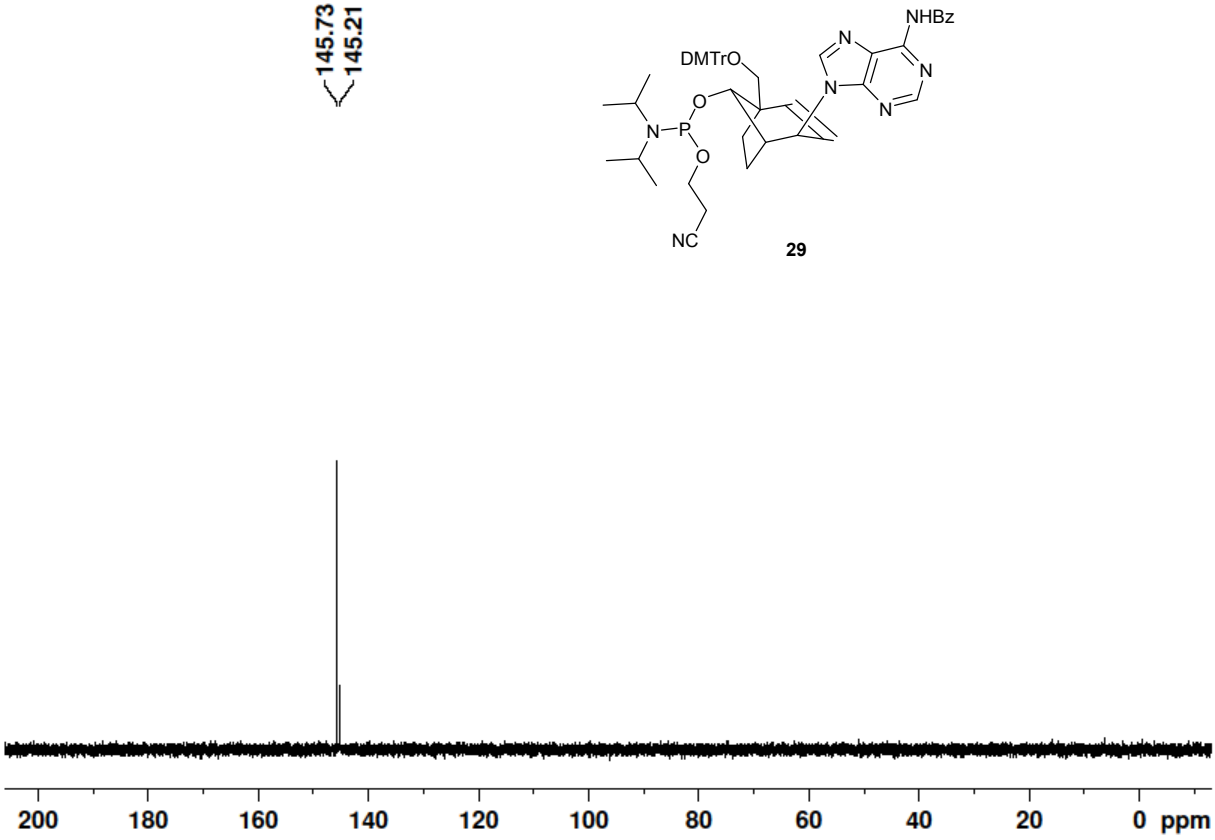
145.73
145.21
NHBz
DMTrO
N
N
N
N
O
N
P
O
NC
29
200
180
160
140
120
100
80
60
40
20
0 ppm

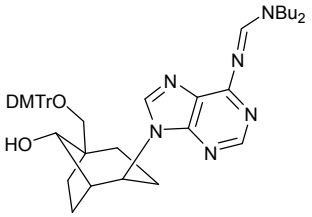
NBu2
N
N
N
N
N
DMTrO
HO

30

10.0 9.5 9.0 8.5 8.0 7.5 7.0 6.5 6.0 5.5 5.0 4.5 4.0 3.5 3.0 2.5 2.0 1.5 1.0 0.5 ppm
1.0 1.0 1.0 2.1 1.8 4.4 1.1 4.1 1.0 1.0 6.2 2.1 2.0 1.0 1.3 1.0 1.0 1.0 2.0 1.2 1.0 1.0 6.1 1.1 4.2 6.1

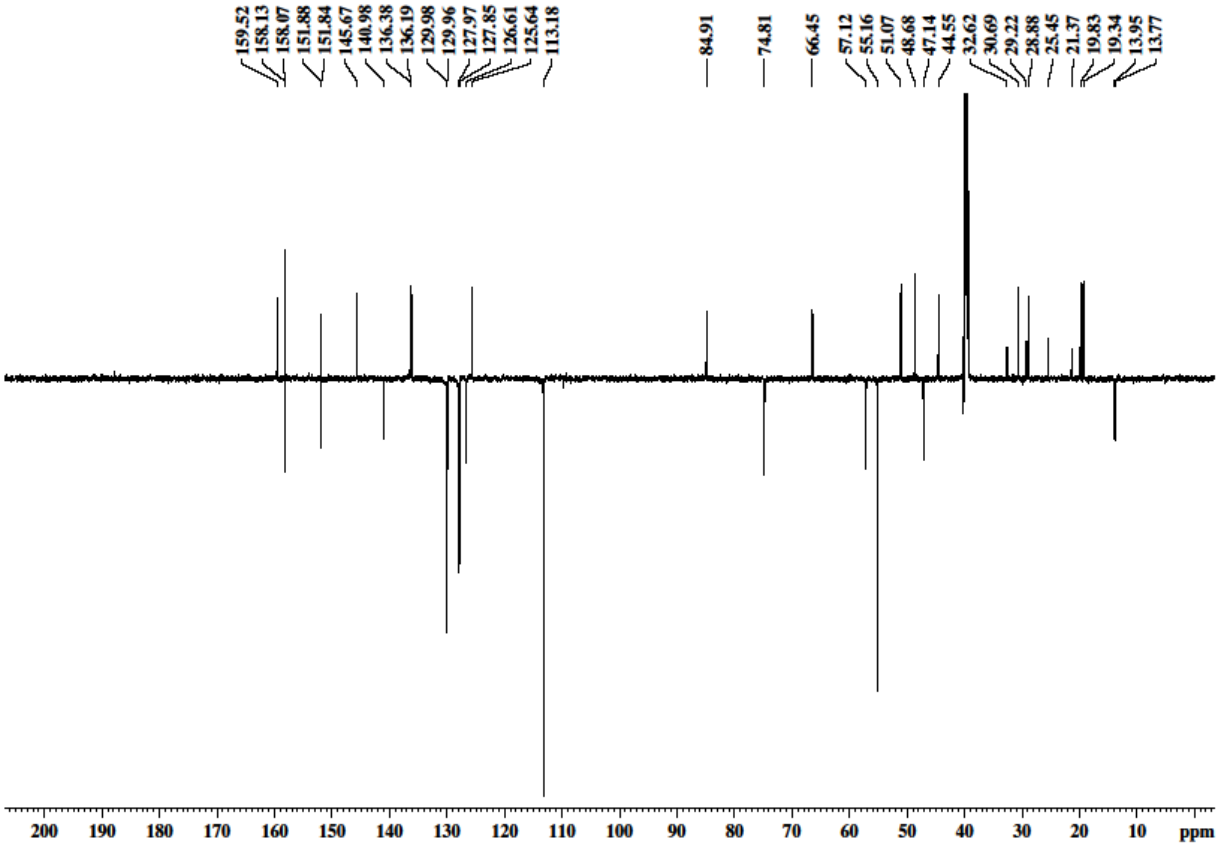
159.52
158.13
158.07
151.88
151.84
145.67
140.98
136.38
136.19
129.98
129.96
127.97
127.85
126.61
125.64
113.18
84.91
74.81
66.45
57.12
55.16
51.07
48.68
47.14
44.55
32.62
30.69
29.22
28.88
25.45
21.37
19.83
19.34
13.95
13.77
200 190 180 170 160 150 140 130 120 110 100 90 80 70 60 50 40 30 20 10 ppm

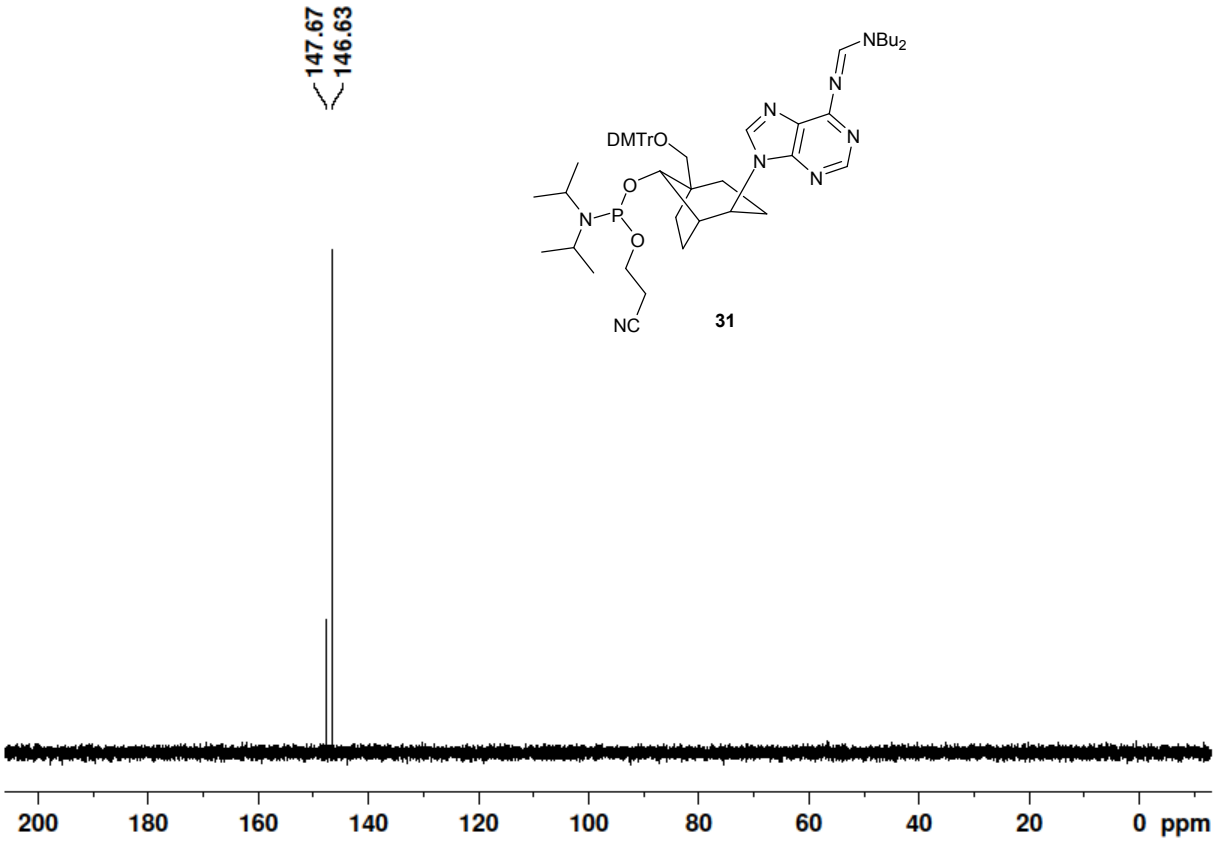
147.67
146.63
NBu2
N
N
N
N
N
DMTrO
O
N
P
O
NC
31
200
180
160
140
120
100
80
60
40
20
0 ppm

Figure **S7**. In contrast to the preferred conformation of cANA, LCeNA should adopt a conformation that situates the nucleobase in an "axial-like" orientation due to repulsion of the hydrogen atom of the -CH_2CH_2- bridge and the hydrogen atom vicinal to nucleobase

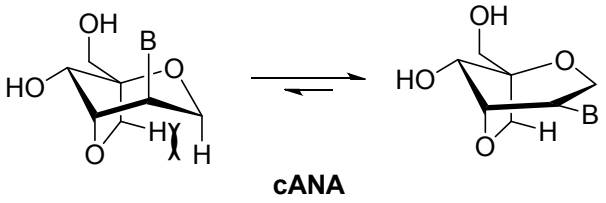

cANA

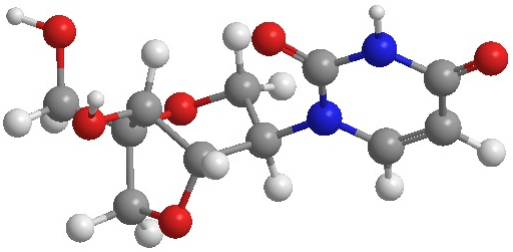

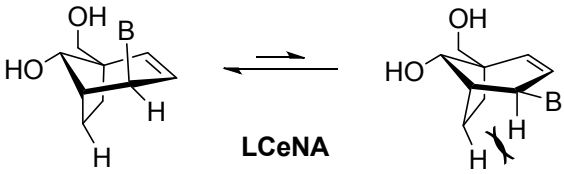

LCeNA

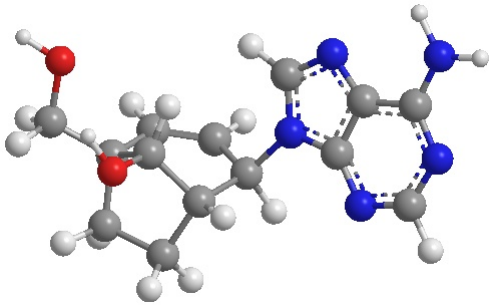

.

Results of molecular dynamic calculations

The values of α, γ, and δ torsion angles calculated for normal oligonucleotide and oligonucleotides including one (A5) and three (A3, A5, A8) modifications differed.

In normal chain 5'-G1–C9-3', the values of α torsions for individual residues averaged employing calculated snap shot geometries ranged from 263° to 285°. The averaged γ torsions ranged typically from 65° to 81°, but for the G1 and C9 terminal residues it was 110° and 54°, respectively. The overall values of α and γ torsions were typically ~280° and ~70°, except shortly lasting and rarely occurring concerted α-γ switches when α/γ values ~280°/~70° changed to ~150°/~190° (Figure **S7**). The averaged δ torsion ranged for most of residues from 78° to 82°. However, when δ close to ~120° for some period occurred (A8 residue) or δ fluctuating fast between ~80° and ~120° occurred (C9 terminal residue) the averaged δ torsion value was 106° and 120°, respectively. The typical values of α, γ, and δ torsion angles calculated for normal 5'-G1–C9-3' chain were characteristic values indicating normal A-RNA structural class of RNA oligonucleotide[3].

In 5'-G1–C9-3' chain containing one modified residue A5, the averaged value of α, γ, and δ torsion calculated for A5 residue was 240°, 63°, and 54°, respectively. The distribution of α values in modified A5 was significantly broader and the averaged α value smaller compared to normal A5 residue (Figure **S13**). The modified A5 residue possessed also one other distinguishable feature; the averaged value of γ torsion (63°) was larger than averaged value of δ torsion (55°) while in normal residues was δ larger than γ torsion. The structure of U4 and U6 residues neighboring to modified A5 residue was largely perturbed, namely owing to frequent occurrence of the α/γ switches (Figure **S7**). The distributions calculated for α torsion in U4, U6 and C7 residues are bi- or even tri-modal while α torsions in normal chain typically possessed single-mode distribution centered at ~280° (Figure **S13**). The A5 modification thus introduced structural disorder particularly to the neighboring residues while the modified residue itself was structurally rigid and abnormal compared to regular residues in normal RNA oligonucleotides.

The values of α, γ, and δ torsion calculated for modified A3, A5 and A8 residues in 5'-G1–C9-3' chain containing the three modifications were again characteristic. The averaged value of α torsion for A3, A5 and A8 modified residue was 268°, 245°, and 240°, respectively. The distributions of α torsions for three modified residues broadened compared

to those for normal residues (Figure **S13**). The averaged values of δ torsions calculated for A3, A5 and A8 modified residues 52°, 55°, 55° were smaller than the averaged values of γ torsions 56°, 63°, 64°. All the three modified residues were structurally more rigid and abnormal compared to normal residues. The structural disorder of normal residues neighboring to the modified residues was large. Notably, the fast and concerted fluctuations of α and γ torsions were calculated particularly for normal U6 residue (Figure **S8**). We therefore assume that structural disorder/instability of normal residues introduced by modifications may be cumulative for some residues that may depend on sequential positioning of modifications.

Figure **S8**.

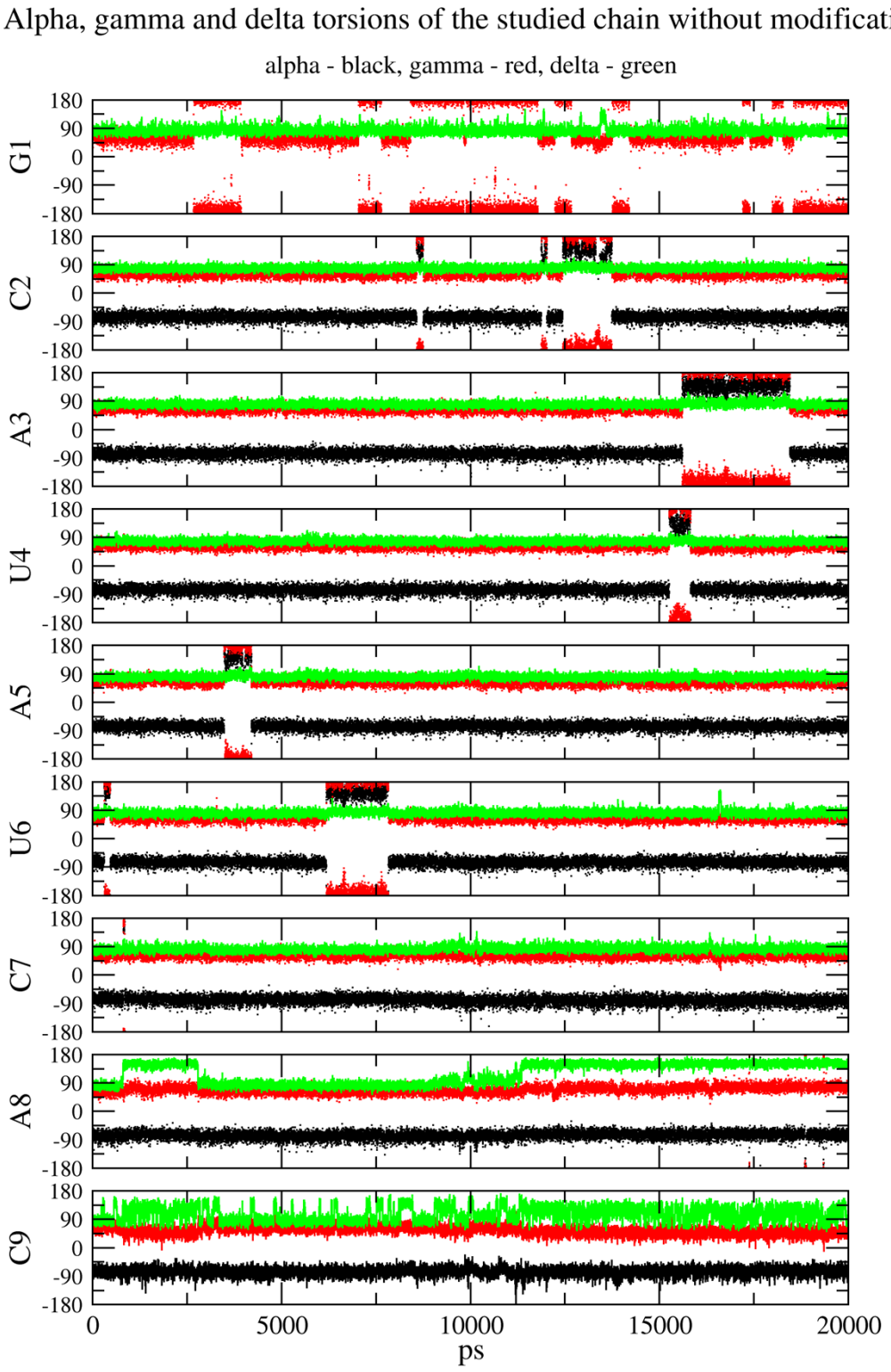
Alpha, gamma and delta torsions of the studied chain without modifications
alpha - black, gamma - red, delta - green
G1
C2
A3
U4
A5
U6
C7
A8
C9
180
90
0
-90
-180
0
5000
10000
15000
20000
ps

Figure **S9**.

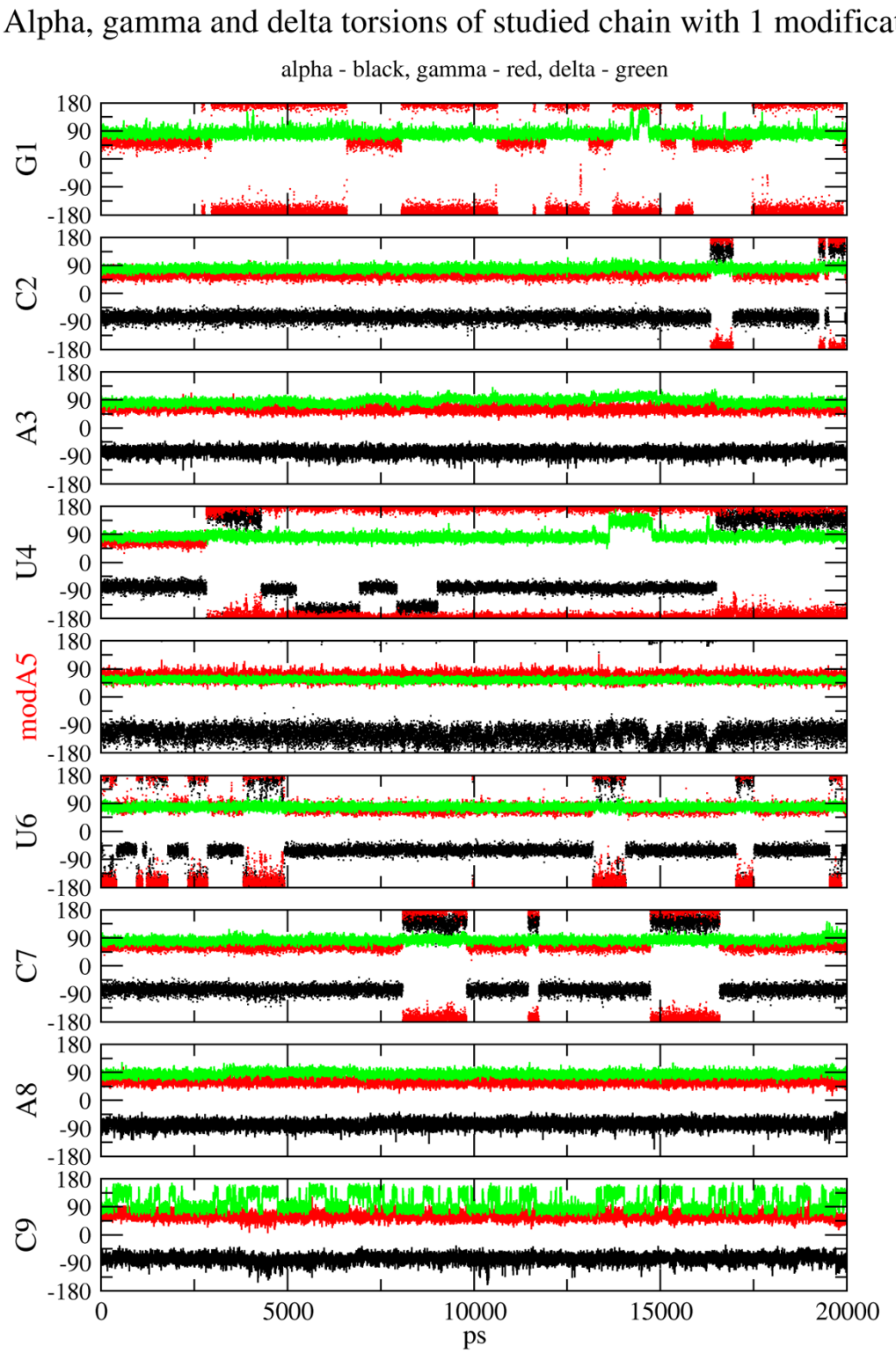
Alpha, gamma and delta torsions of studied chain with 1 modification
alpha - black, gamma - red, delta - green
G1
C2
A3
U4
modA5
U6
C7
A8
C9
180
90
0
-90
-180
0
5000
10000
15000
20000
ps

Figure **S10**.

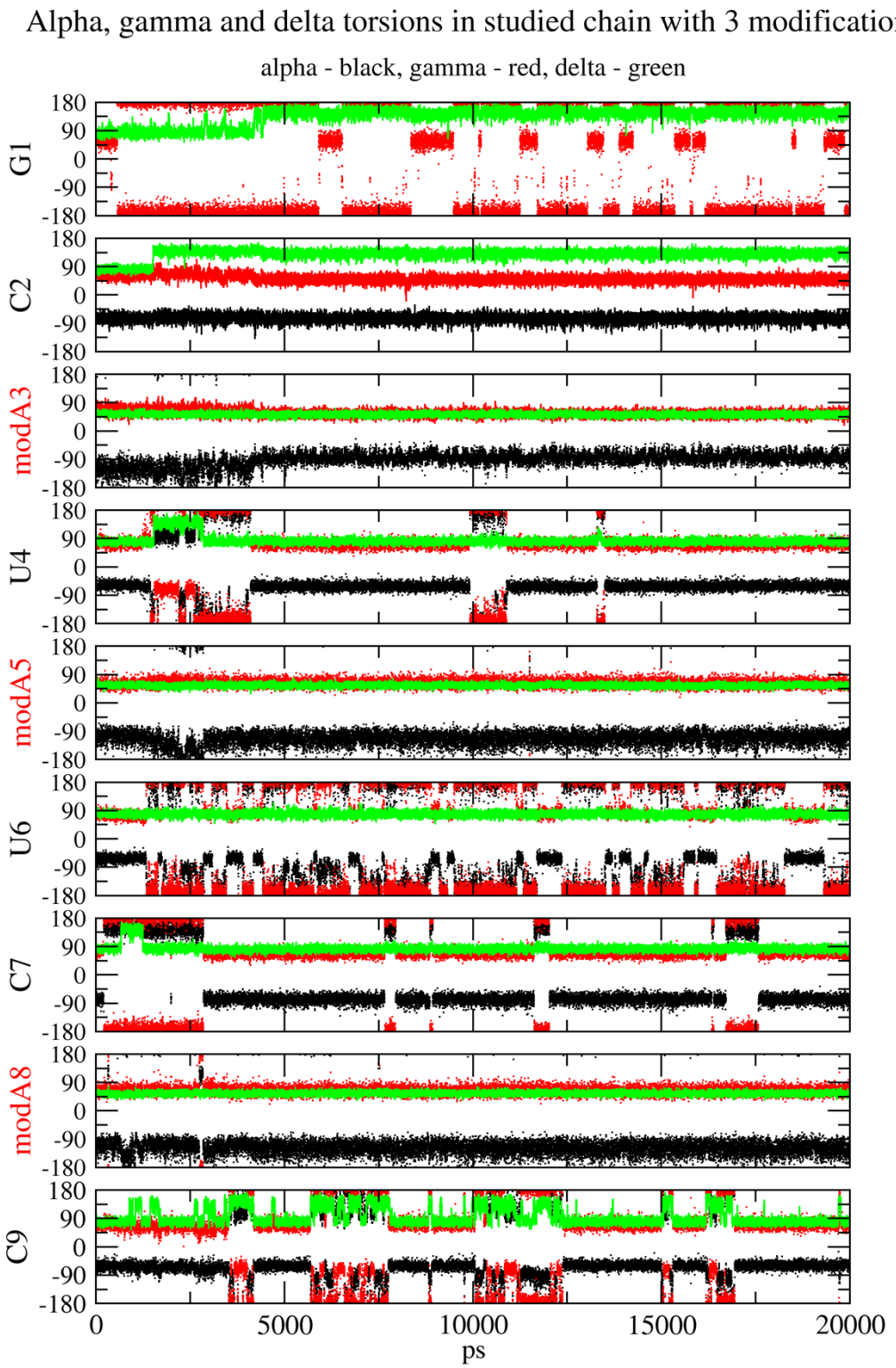
Alpha, gamma and delta torsions in studied chain with 3 modifications
alpha - black, gamma - red, delta - green
G1
C2
modA3
U4
modA5
U6
C7
modA8
C9
180
90
0
-90
-180
0
5000
10000
15000
20000
ps

Figure **S11**.

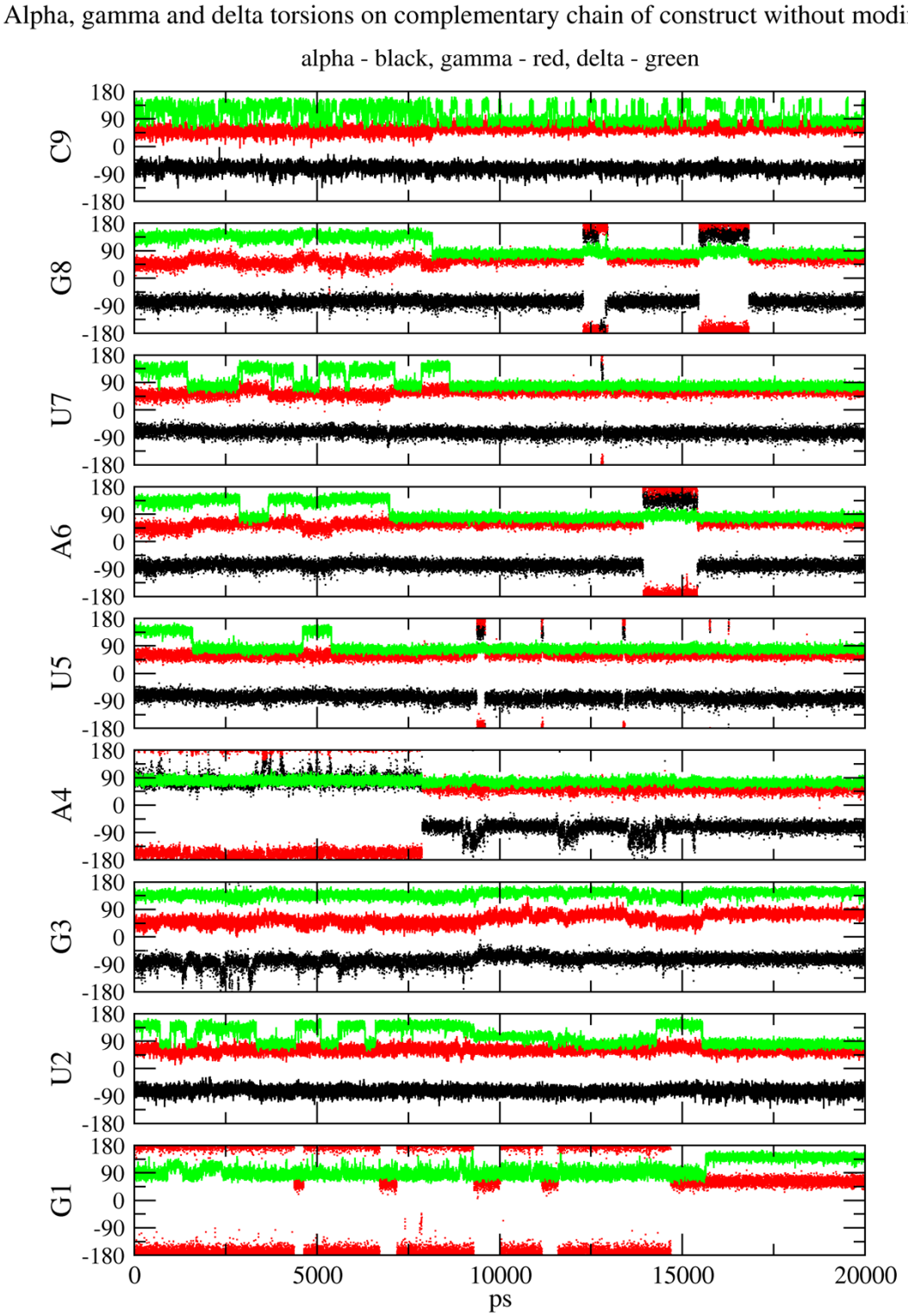
Alpha, gamma and delta torsions on complementary chain of construct without modifications
alpha - black, gamma - red, delta - green
C9
G8
U7
A6
U5
A4
G3
U2
G1
180
90
0
-90
-180
0
5000
10000
15000
20000
ps

Figure **S12**.

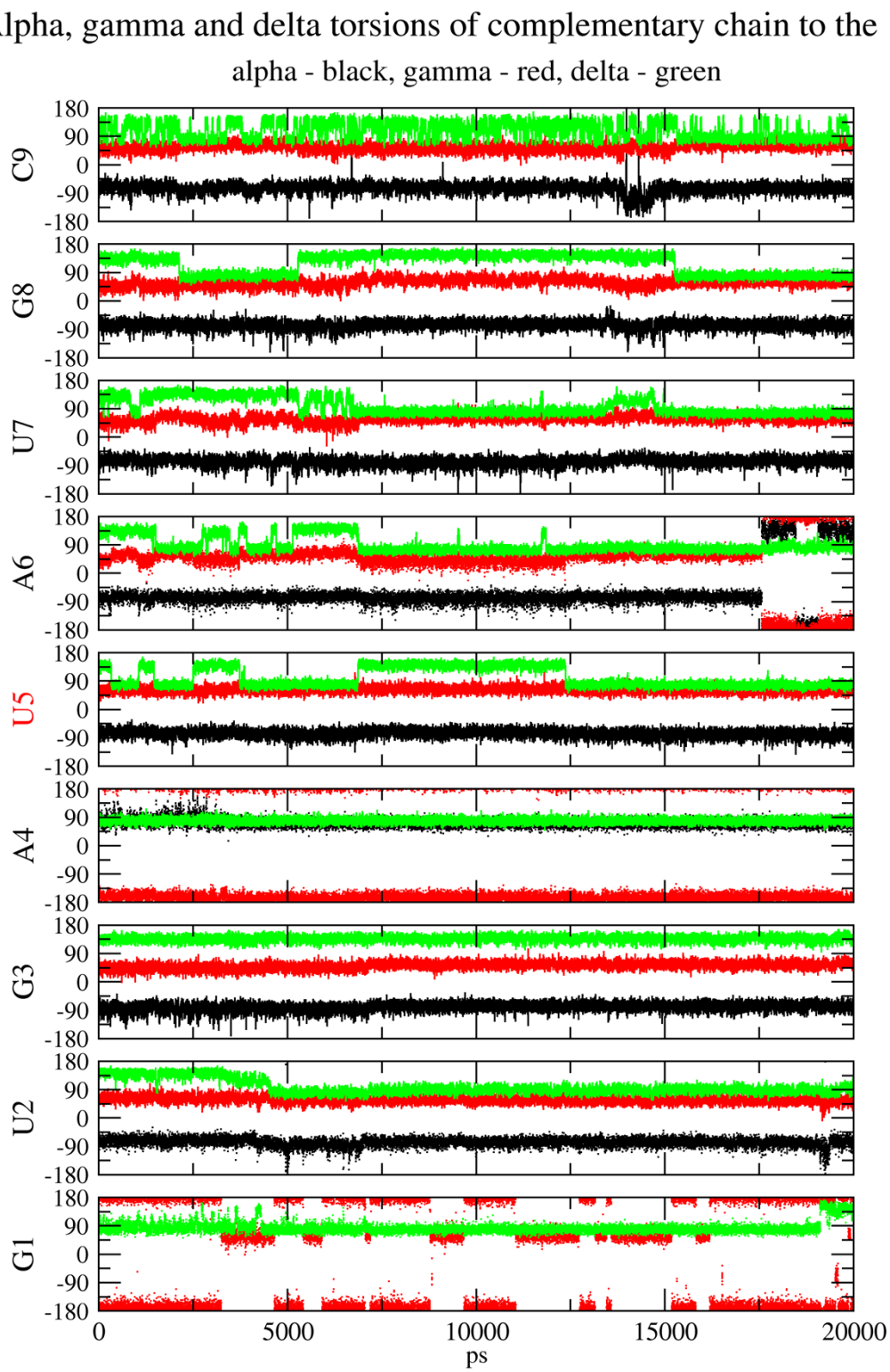
Alpha, gamma and delta torsions of complementary chain to the 1 mod
alpha - black, gamma - red, delta - green
C9
G8
U7
A6
U5
A4
G3
U2
G1
180
90
0
-90
-180
0
5000
10000
15000
20000
ps

Figure **S13**.

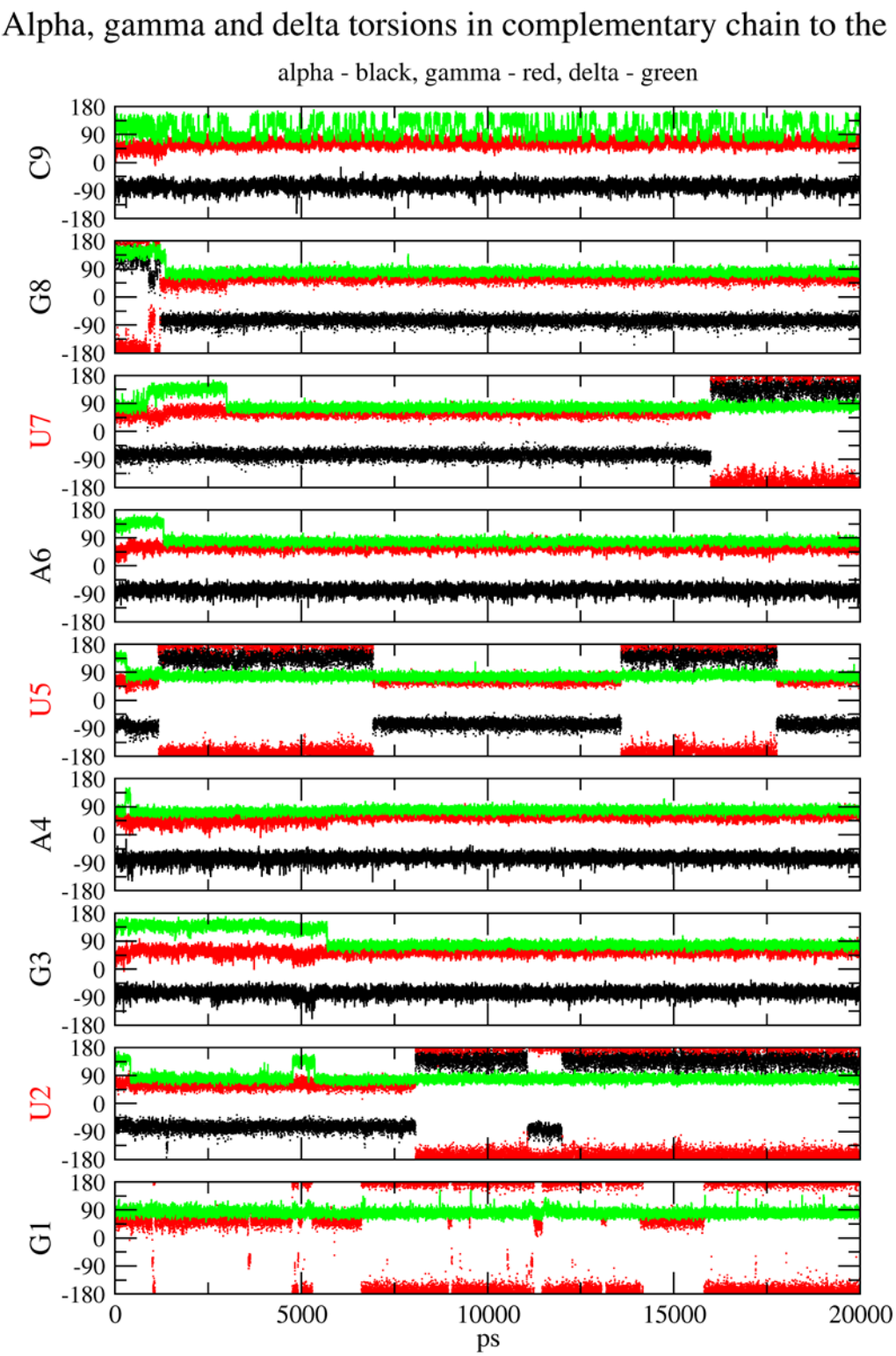
Alpha, gamma and delta torsions in complementary chain to the 3mod
alpha - black, gamma - red, delta - green
C9
G8
U7
A6
U5
A4
G3
U2
G1
180
90
0
-90
-180
0
5000
10000
15000
20000
ps

Figure **S14**. The distributions of alpha, gamma and delta backbone torsion angles calculated for oligonucleotides including zero, one and three modified units.

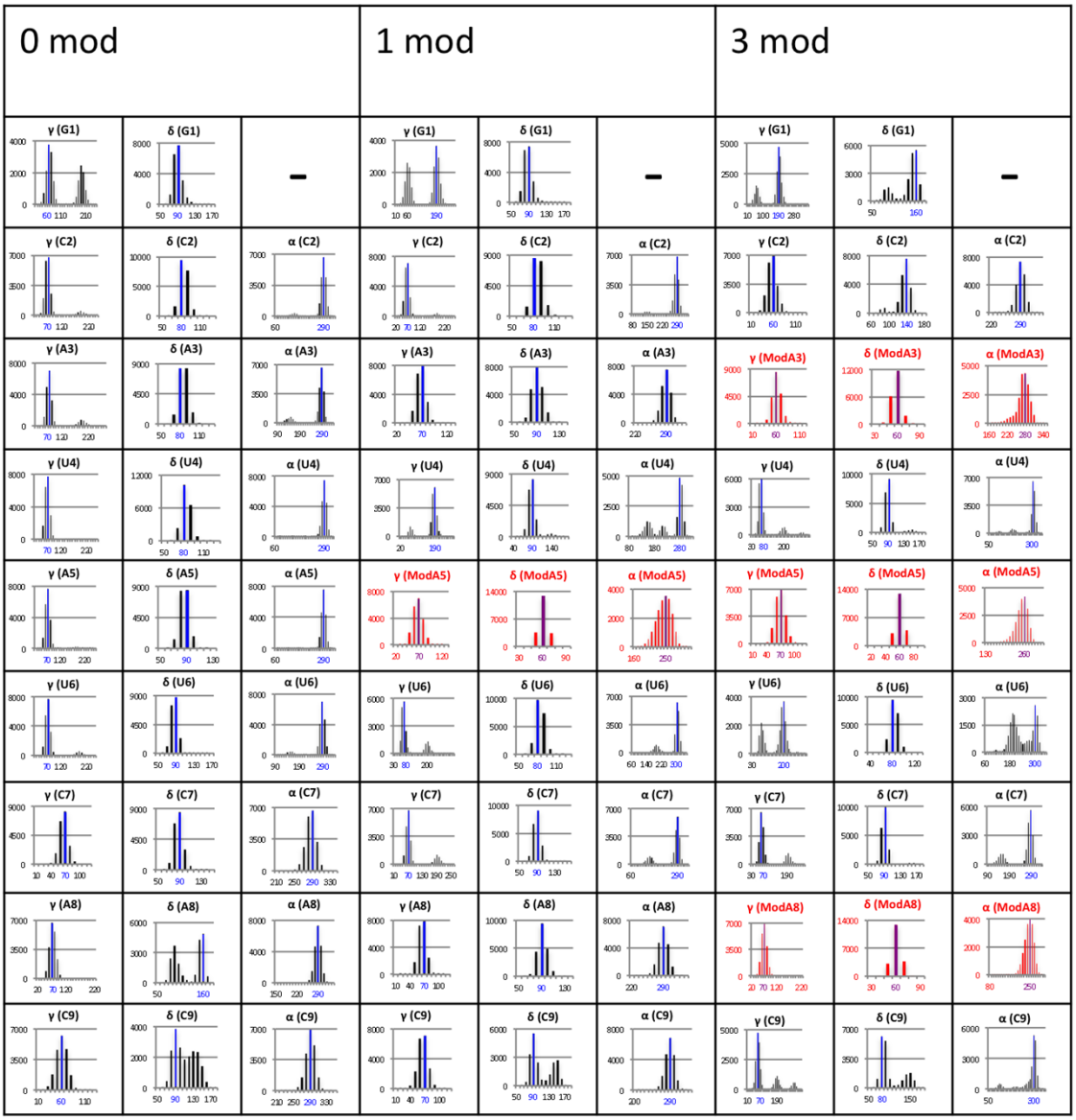

Conformational analysis of 25 and results of the DFT calculations

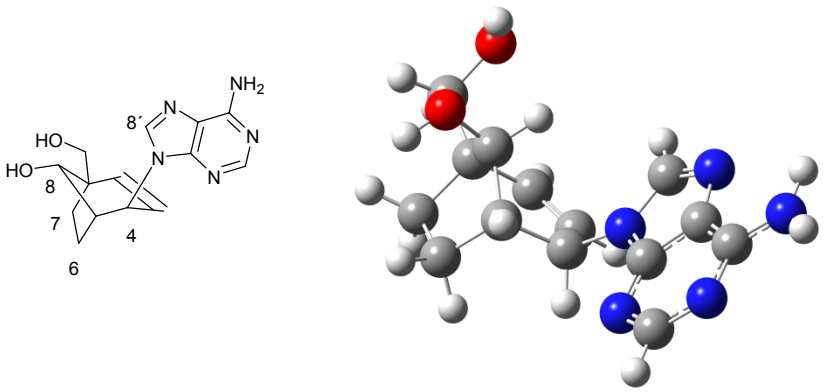

Table **S3**. Calculated (DFT calculations, B3LYP/6-31+G(d,p)) and experimental spin-spin coupling constants for compound **25**.

Interaction	*J* experiment (Hz)	*J* Gaussian (Hz)
H2-H3	9.5	9.3
H3-H4	3.9	4.1
H4-H5	-	2.5
H5-H8	-	1.0
H5-H6ex	7.9	7.9
H5-H6en	-	0.7
H6ex-H7en	2.4	2.3
H6ex-H7ex	10.5	10.8
H6en-H7en	9.2	9.6
H6en-H7ex	6.2	4.8

Computational details of optimized structure of compound **25**. DFT calculations were done using this method: B3LYP/6-31+g(d,p) in vacuum.

Atomic number	x	y	z
6	1.956631	-0.051852	0.892192
6	1.074884	1.095917	0.371626
6	0.343986	0.634668	-0.917389
6	1.281699	-0.116244	-1.834443
6	2.537629	-0.410261	-1.475890
6	3.122463	-0.012937	-0.130782
6	3.466896	1.507515	-0.169484
6	2.100139	2.223537	0.050307
8	2.376509	0.110819	2.247824
6	4.329235	-0.877775	0.246374
8	4.016945	-2.265127	0.359784
7	-4.635308	0.826181	0.393126
6	-3.734368	1.787603	0.127257
7	-2.449541	1.651728	-0.218953
6	-2.093104	0.360530	-0.290657
6	-2.912875	-0.745793	-0.045935
6	-4.248128	-0.460539	0.310497
7	-0.857795	-0.164643	-0.617298
6	-1.005530	-1.539317	-0.547696
7	-2.215638	-1.928749	-0.212373
7	-5.156974	-1.434582	0.559971
1	1.441291	-1.015337	0.881390
1	0.327835	1.408205	1.106384

1	-0.042172	1.526434	-1.425476
1	0.900376	-0.398188	-2.813400
1	3.191754	-0.930443	-2.173157
1	4.178423	1.753330	0.629471
1	3.941798	1.790929	-1.112741
1	1.792672	2.800323	-0.827292
1	2.158443	2.939965	0.876800
1	2.655740	1.022724	2.403709
1	5.090845	-0.807133	-0.538334
1	4.771393	-0.503456	1.177857
1	3.559238	-2.406048	1.199106
1	-4.103281	2.807064	0.207091
1	-0.180482	-2.201325	-0.770060
1	-4.868214	-2.399578	0.584022
1	-6.073840	-1.172858	0.886597

Figure **S15**. The allylic rearrangement of the compound **22a** in DMSO-d_6 was monitored by ^{1}H NMR spectroscopy within several days at room temperature. Only double bond region, where the most significant changes have been noticed, is shown. As a result, the mixture of the starting compound **22a** and the product **22** was obtained. This process provides an opportunity to recycle the undesired azido derivative **22a** and so that to increase the yield of the previous reaction.

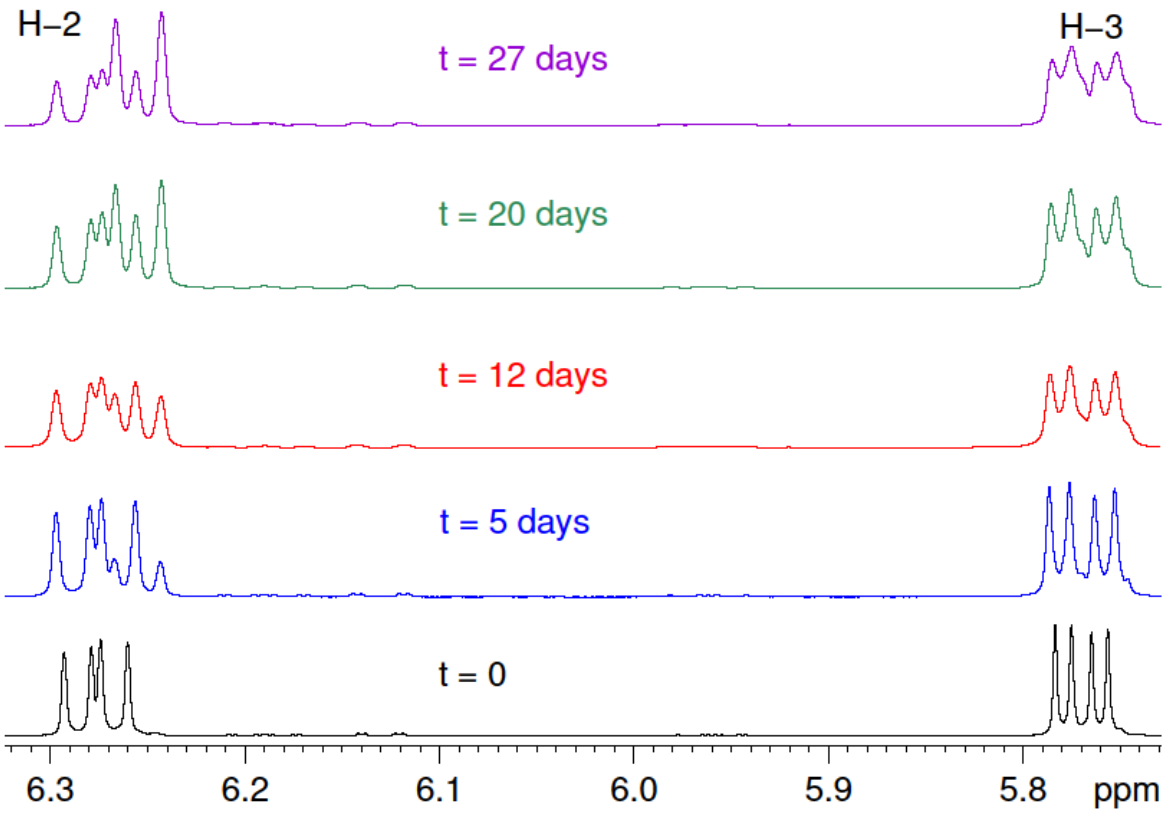

Figure **S16.** A overlaid structural model of nucleoside **25** (LCeNA mononer unit, green) with adenosine (yellow) in C3'- endo conformation

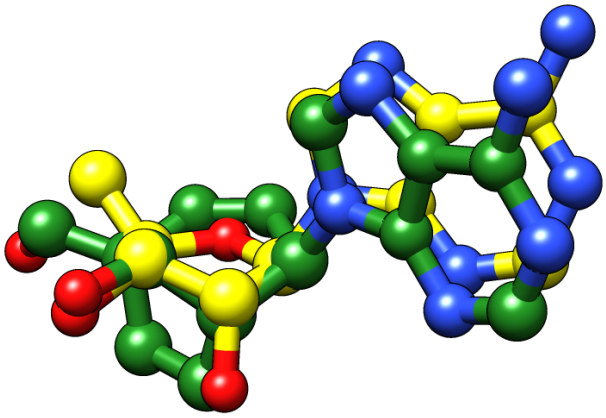

References:

1. F. H. Wu, R. Hong, J. H. Khan, X. F. Liu and L. Deng, *Angew. Chem. Int. Ed.* 2006, **45**, 4301-4305.
2. M.-H. Filippini, R. Faure and J. Rodriguez, *J. Org. Chem*. 1995, **60**, 6872-6882.
3. B. Schneider, Z. Morávek and H. M. Berman, *Nucleic Acids Res.* 2004, **32**, 1666-1667.